UNIVERSITY OF BATH

The Design Of A Novel Repair Satellite Technology

Sub-System Focus: Satellite Attitude Control System

By Candidate : 11189

Word Count: 6857

Contents

List of Figures

List of Tables

1 Introduction and Overview

1.1 Project Introduction And Context

The future of the space industry at its core is linked with sustainability. Whilst space becomes more congested and costly to operate in, it is simultaneously becoming more imperative in modern life (from communications to scientific exploration).

Currently, satellites launched are not designed to be repaired thus once they fail or reach end-of-life they are replaced at a huge cost both economically and environmentally. As of 2024, there were over 3000 non-operational satellites in orbit[1], a vast amount of orbital debris that could impede future space endeavours.

This fundamental issue is forever increasing (particularly due to the new mega-constellations) sparking a vaster desire for an efficient and reliable in-orbit servicing technology that can inspect, repair and upgrade satellites to expand mission lifetime. While numerous concepts have been proposed , no viable solution has yet been launched.

This project, developed in collaboration with DSTL, aims on developing an autonomous robotic repair system aimed at enabling efficient, low-cost satellite servicing with limited human intervention. Doing so, operational costs should be reduced and mission lifespans extended. Ultimately laying a revolutionary groundwork for a reliable future for all space operations.

1.2 Project Objectives And Scope

The core objective of this project is to develop a proof-of-concept robotic system fully capable of performing in-orbit satellite repairs using widely available off-the-shelf components in a magnitude of orbits. The system must safely identify, easily access and replace faulty components with little to no risk of additional damage to the satellite being repaired.

The exact goals as directly requested by the client (DSTL), include:

- **Design a robotic manipulator system** (e.g., robotic arm or grabber) capable of controlled interaction with a satellite component in space.
- **Sensing technology** (such as cameras or proximity sensors) to detect and locate malfunctioning components accurately.
- **Select and justify off-the-shelf components** for mechanical, electrical, and sensing subsystems, based on cost-effectiveness, performance, and space-readiness.
- **Simulate a satellite-to-satellite interaction** to evaluate positioning, access techniques, and repair operations in a representative orbital servicing scenario.
- **Minimise the risk of damage** to the damaged satellite during servicing through considered manipulation strategies and system constraints.

A secondary objective requested is to design the repair system itself in a way that avoids becoming future orbital debris once the end-of-life has been reached.

Commercially, the project will explore the potential for a third-party service as a more cost-effective solution and alternative to satellite replacement.

1.3 Design And Development Approach

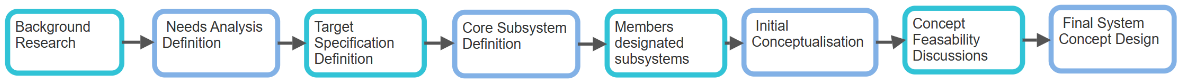

Figure 1: Timeline of the design process

1.3.1 Background Research

Research was primarily done to fully grasp the current challenges in satellite repair servicing, specifically the issue of space debris and lack of any in-orbit repair solutions. This provided the foundations in defining realistic and essential needs and targets for the project.

1.3.2 Needs Analysis And Target Specification Definition

Using the research, the needs analysis (See appendix A) was created identifying the crucial and necessary requirements of the project separated into technical , commercial and ethical needs. This analysis defined the key priorities for the design.

Subsequently, the target specification (see appendix B) was formed. Laying out all the desired capabilities of the system and acted as a benchmark from which all subsystems were created and solutions were compared against.

1.3.3 Core Subsystems

Using both the technical specification and needs analysis a general system architecture was developed outlining the primary technical functions that the system must meet and how these systems will fundamentally interact with each other.

Three main subsystems were devised:

- **Launch And Orbital Approach** The mission planning and orbit determination in order for repair satellite to effectively rendezvous with target satellite.
- **Satellite Attitude Control And Capture** Control systems and attitude control methods needed to control stability both in normal and repair operational modes.
- **Modular System And Arm** Modular design to allow for efficient, seamless repairs and a modular arm end effector to interact with the modular system and allow for future unique repairs

The three core subsystems will form the heart of the overall system architecture. Whilst each subsystem is critical for an independent function in the final systems operation, they are very interdependent and must operate effectively together.

The interaction between the fundamental subsystems are implemented in the block diagram visible in Figure 2.

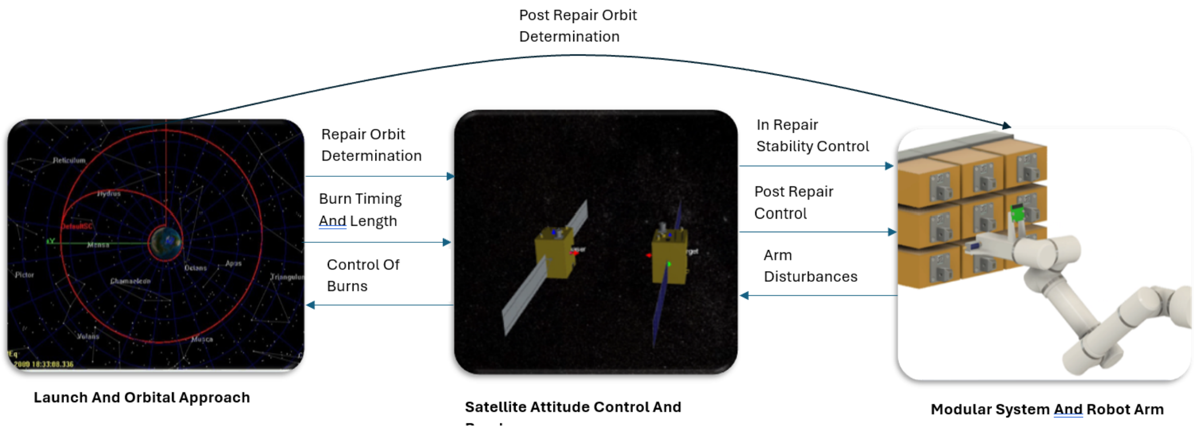

Figure 2: Core Subsystems And Basic Interactions Block Diagram

1.3.4 Initial Conceptualisation And Feasibility

An iterative design approach was done during the idea conceptualisation, being benchmarked against the target specifications along the way in order to test for feasibility. Idea iterations and approach examples can be seen in Appendix C.

1.4 Final System Concept Overview

The overall system was designed to perform autonomous in-orbit repair on malfunctioning satellites using a novel modular system that can be implemented on new non-legacy satellites. Focusing on modularity, autonomy, and control systems to implement a safe and efficient repair.

The 3 core subsystems were decomposed into specific technical problems that need to be solved based on the derived technical requirements.

The block diagram shown in Figure 3 illustrates the technical problems that need to be involved during the launch and orbital approach. This phase will encompass the calculation of the transfer orbit needed and the burn durations needed to get the repair satellite from its current orbit into the transfer orbit.

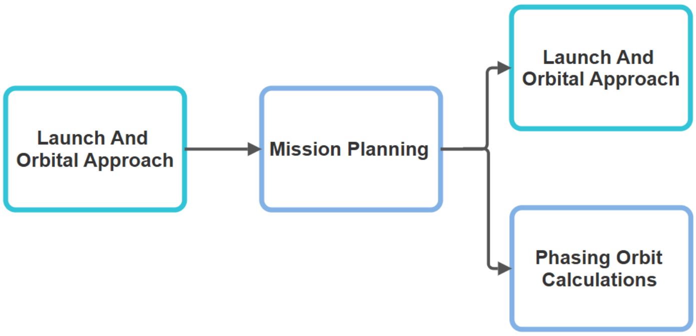

Figure 3: Block Diagram of Orbital Approach Subsystem

Figure 4 presents the technical breakdown of the attitude and rendezvous control subsystem which begins once the repair satellite is within docking distance of the target. This phase will involve lidar distance measurements, a series of rendezvous control systems for the thrusters to control the approach to the target, the docking method to secure the two satellites and the stability/ attitude control system to keep the repair satellite stable for any disturbances caused during the repair process.

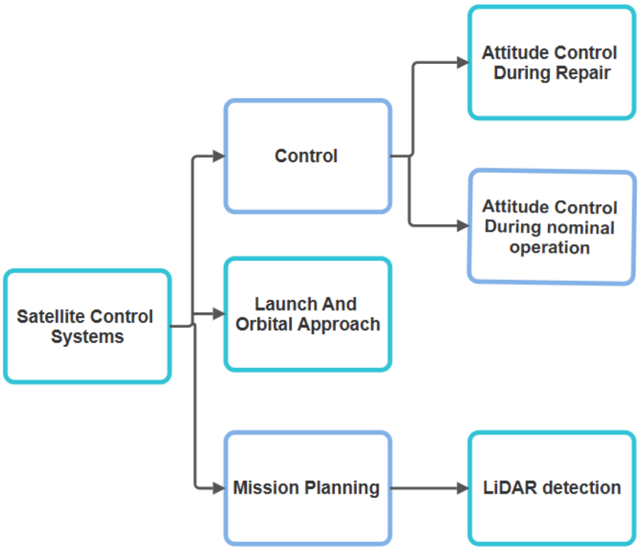

Figure 4: Block Diagram of Rendezvous and Attitude Control Subsystem

The final phase, detailed in Figure 5, shows the modular system and robotic arm that will perform the repair. A modular chassis system with a QR code for position detection is used along with a camera on the robot arm. A unique end effector and gripping method is designed to remove faulty 'units' and replace or upgrade with working ones.

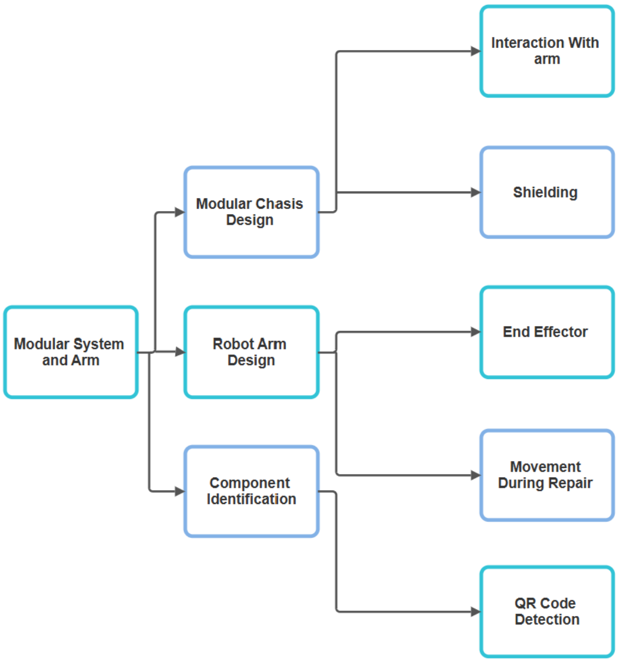

Figure 5: Block Diagram of Control Process

The mission has two key functional flows. Primarily the orbital approach and rendezvous and secondly, the in orbit repair execution. Figure 6 outlines the process to achieve a stable and precise alignment with the target satellite.

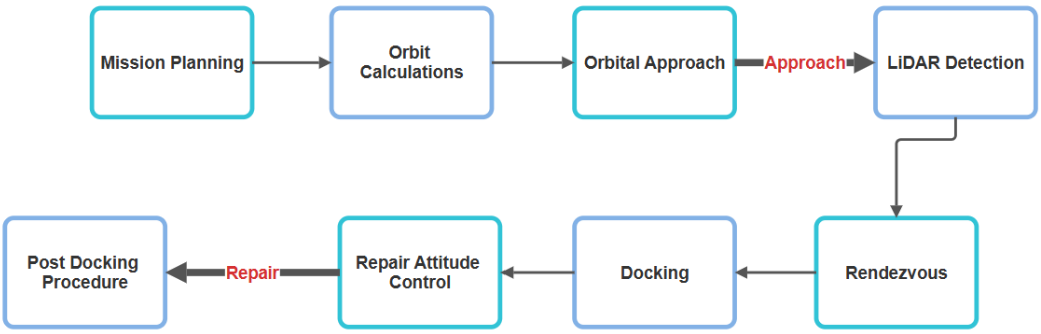

Figure 6: flowchart of rendezvous process

In contrast, Figure 7 shows the repair process, detailing the steps taken by the robotic arm and visual computing to execute the repair whilst docked.

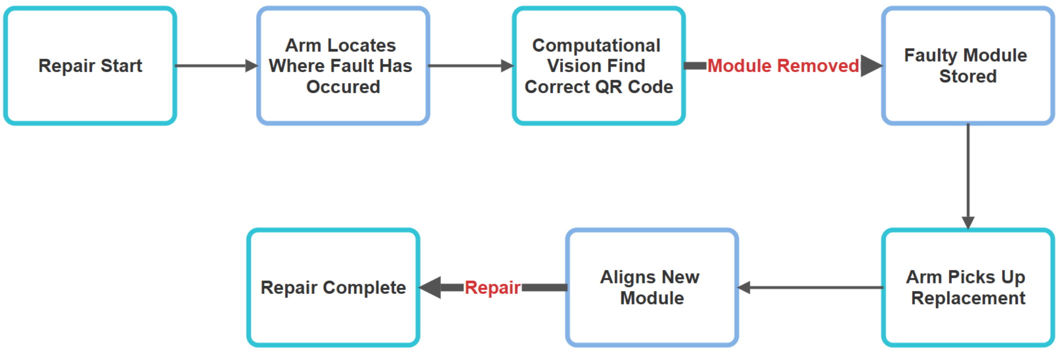

Figure 7: flowchart of Repair

1.5 Specific Sub-System: Attitude Control System

1.5.1 Overview of subsystem role

The SACS is a critical component in nearly every satellite platform, its primary function is to measure and control the attitude of the satellite in a way that best fits its unique mission requirements (such as pointing payload or instruments towards Earth). Based on the mission requirements of the repair satellite, the SACS role is to keep the repair satellite stable despite any disturbances such that the repair takes place in optimum conditions.

Attitude control becomes particularly important in low Earth orbits (LEO), where satellites are exposed to a vaster amount of external disturbances as a consequent of the satellite being close to Earth such as atmospheric drag, radiation pressure and forces that are a consequence of the satellite being in the Earths magnetic field [2]. All of these environmental disturbances in combination with forces caused by the movement of the arm will cause significant deviation in orientation if not effectively managed possibly leading to an unsuccessful repair thus making the need of a responsive and robust SACS imperative for mission success.

Attitude control and determination rely on two key physical components, primarily sensors that detects and measures a physical quantity in this case angular rate and attitude and converts it to an electrical signal for the control system to interpret [3]. Secondly, actuators that takes electrical commands from the control signal and produces a physical response such as torque to change the satellites orientation/attitude [2].

This report focuses on the design procedure and evaluation of an SACS with emphasis on the performance targets, design constraints, standards and design trade-off analysis leading to the final design. The aim is to develop an SACS that delivers three-axis stabilisation with high accuracy and fast response times with in built redundancy in case of failures.

The design process considers a range of actuators and sensors and evaluates them against key criteria guided by key standards (NASA, ESA etc).

1.5.2 Integration of Subsystem

The attitude control systems are unique in that they are imperative in both the orbital approach and the repair itself. These control subsystems will integrate with others as detailed in Table 1. The SACS must react effectually to torques generated from docking and the repair process whilst no impeding any functionality

Subsystem	Input or Output	Interaction with Control Systems
Orbit Planning	Input	Must be on correct orbital path to dock where stability is crucial.
LiDAR Positioning	Input	Provides real-time distance measurements to the target satellite for precise approach control.
Docking System	Output	Relies on accurate positioning from the SACS to engage docking mechanisms safely.
Arm Movement	Input	Large, fast disturbances from arm motion require rapid SACS compensation to maintain attitude.
Arm Stability	Output	Attitude control actively stabilizes the satellite during fine manipulation tasks.
Post-Repair Phase	Output	Ensures controlled and gradual undocking to maintain system stability after repair completion.

Table 1: Integration of Subsystems with the Satellite Attitude Control System (SACS)

2 Design Specification And Evaluation Of System

2.1 Functional Specifications

Functionally, the SACS must maintain the satellites attitude during both normal operation and during repair.

The Key requirements of an efficient and effective SACS require it to measure attitude and angular rates compare them to desired values and produce the exact relevant torque whilst reacting in real time to disturbances [4]. The following block diagram (Figure 8) details the clear flow of sensor inputs and reaction of subsequent actuators in order to make a functional SACS

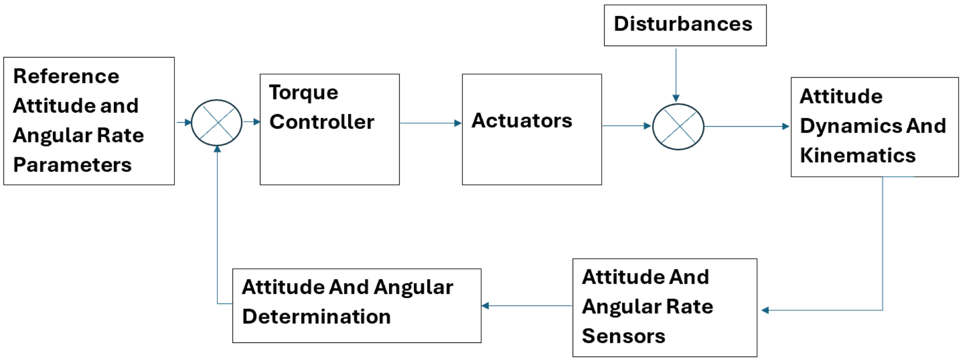

Figure 8: Functional Operation Block Diagram

From this, the high-level requirements of the subsystem that must be completed to formulate a valid and robust solution as outlined in Table 2

Requirement	**Rationale**
Use sensors to measure attitude.	Ensures that amount of torque needed for adjustment can be calculated.
Apply torque through the use of actuators.	Keeps the satellite stable during the repair.
Compensate for all significant external disturbance torques during repair.	Keeps the satellite stable against environmental disturbances (gravity-gradient, solar torques, etc.[5]).
Provide continuous attitude data .	Needed for accurate control.
Provide continuous angular rate data for guidance	Allows accurate control with redundancy.
Redundancy to allow for a single-point failure.	Guarantees mission robustness against faults.

Table 2: Functional Requirements for the Satellite Attitude Control Subsystem (SACS)

2.2 Selection Criteria And Deisgn Constraints

Following from the functional requirements, each can be translated into precise, real-world design constraints that affect the selection of the actuators and sensors all of which must be met during the design process to create an effective SACS for the repair mission.

Table 3 summarises the mission-driven selection criteria/constraints used to evaluate design alternatives for the actuators and sensors that could be implemented in the repair satellite. Each criterion represents a critical consideration that must be taken to implement the SACS.

Criterion	Mission-Level Justification	Importance for Mission
Torque	Must provide exact control torque to counter disturbance loads and maintain stability during repair.	High
Three-axis control	Needs to control for x, y and z axis.	Very High
Disturbance Resistance	Must react to disturbances caused by external forces and the movement of the arm.	High
Precision Pointing	Must be accurate enough such that satellite is fully stable.	High
Mass & Volume	Cannot be excessively large such that launch mass is not exceeded or compromises the repair mission itself.	Medium
Power Demand	Should operate within the limited power budget available across all mission phases, including peak manoeuvring.	Medium
Reliability	Requires redundancy so that a single component failure does not jeopardize the servicing mission.	High
Integration Simplicity	Should interface cleanly with other subsystems.	Medium
Thermal Compatibility	Needs to operate within the spacecraft's thermal control margins without causing failures.	Medium
Orbit Suitability	Needs to be able to operate in both near Earth and far Earth orbits.	High

Table 3: Mission-Driven Selection Criteria for Attitude Actuators and Sensors

2.3 Actuator Design Alternatives

In order to fulfil the functional requirements and meet the performance objectives of the SACS, an array of actuator and sensor alternatives were considered. This section explores the use of different viable actuator and sensor types for the mission and evaluates their suitability in the context of the repair mission. Alternatives are assessed based on mission-specific selection criteria (Table 3) .

2.3.1 Reaction Wheels

Reaction wheels (RWs) are a very commonly used actuator in SACS design. RWs store angular momentum in a flywheel in order to exert torque on a satellite via the conservation of angular momentum [6]. When the wheel's spin rate is altered by a DC motor, the satellite reacts with an opposite torque equal in size.

$$\mathbf{T}_{\mathrm{RW}} = I_{\mathrm{wheel}}\,\dot{\omega}_{\mathrm{wheel}} \tag{1}$$

where I_{wheel} is the wheel moment of inertia (MOI) and $\dot{\omega}_{\mathrm{wheel}}$ is its angular acceleration [7], showing that as the wheel's angular acceleration changes, a proportional torque is exerted in the satellite. Reaction wheels are the cornerstone of high-precision SACS design as they deliver smooth and continuous torque without any propellant, and are very high precision pointing in the range of micro-radians [8].

In the context of on-orbit servicing, medium-class wheels (0.02–0.05 N·m continuous torque, 0.5–1 N·m·s momentum capacity [9]) can suffice in countering environmental disturbances (gravity-gradient and solar-torque disturbances) as well as disturbances caused by the arm during the repair process [5].

The RWs despite their smooth torque output can saturate at a maximum torque defined by the maximum speed (usually 4000 - 6000 RPM [10] thus will need another way of generating torque (usually thrusters) to desaturate the wheels

Table 4 summarises the key features of RWs and how they meet the mission-specific criteria with qualitative ratings and notes on implementation.

Criterion	**Rating**	**Key Note**	**Ref.**
Torque	High	0.02N·m continuous, up to 0.05N·m peak	[9]
Three-Axis Control	High	Tetrahedral layout ensures full X–Y–Z control and redundancy in case of failure	[10]
Disturbance Rejection	Medium/High	large disturbances needs torque impulse to desaturate	[8]
Precision Pointing	Very High	In micro-radian range	[8]
Mass & Volume	Low/Medium	1 - 5KG per wheel	[8]
Power Consumption	Low/Medium	10-100W	[8]
Reliability	High	10 - 15 years and stored internally	[8]
Saturation Risk	High	Requires periodic desaturation support	[8]
Integration Simplicity	High	Standardised Units	[9]
Thermal Capability	High	Operates in -20 to 60 degrees	[9]

Table 4: Reaction-wheel performance vs. mission criteria

2.3.2 Thrusters

Micro-thrusters are small and compact propellant devices designed to deliver timed, low impulse thrust for attitude control and reaction wheel desaturation [11]. A thruster sized for the mission-specific task will generate $\approx$ 0.5N of thrust at 220-225 seconds specific impulse [12]. This enables controlled momentum dumps all whilst conserving propellant and power [11]. Arrays of thrusters can be arranged to ensure full three-axis control with redundancy, at the expense of environmental and economical cost.

Table 5 evaluates an example micro-thruster against the mission-driven selection:

Criterion	**Rating**	**Key Note**	**Ref.**
Torque Authority	High	0.1–5 mN per thruster—adequate for rapid momentum unloading	[12]
Three-Axis Control	High	Different thruster configurations provides full X–Y–Z coverage and fail-safe	[11]
Disturbance Rejection	Medium/High	thrust counters sustained disturbances and prevents wheel saturation	[11]
Mass & Volume	Low/Medium	Total pack 1.5 kg	[12]
Power Consumption	Low/Medium	zero when idle	[12]
Reliability	High	Minimal moving parts	-
Saturation Risk	High	Essential for periodic reaction-wheel momentum dumps	[11]
Integration Simplicity	High	Standardized modules with unified electrical and plumbing interfaces	[12]
Thermal Capability	High	Rated for –20 °C to +60 °C without performance degradation	[12]

Table 5: Micro-thruster performance vs. mission criteria

2.3.3 Magnetorquers

Magnetorquers are a very common actuator used mainly in Low Earth Orbit (LEO). The magnetorquer generates a magnetic dipole moment which interacts with Earth's magnetic field producing a torque on the satellite [13]. This relationship is defined by the equation 2;

$$\vec{T} = \vec{M}_{\text{dipole}} \times \vec{B} \tag{2}$$

Where $\vec{T}$ is output torque (N.m) , $\vec{M}_{\text{dipole}}$ is magnetic dipole moment ($A.m^2$) and $\vec{B}$ is the magnetic flux density of the Earth (in Teslas) [14]. Thus, showing that when the magnetic field is stronger (closer to Earth), so is the generated torque.

As the satellite moves further away from Earth the torque produced is lower and lower until not enough to provide relevant torque to change attitude. m is usually in the range of 0.2 to 100 $\mathrm{A \cdot m^2}$ [15] and when interacting with B of Earth in LEO it can only produce torque in the milli to micro range. Not enough to react to disturbances efficiently from the arm and very low precision pointing.

Table 6 evaluates magnetorquers against the mission-driven selection

Criterion	**Rating**	**Key Note**	**Ref.**
Torque	Low	In range of micro N.m	[15]
Three-Axis Control	Medium	At least three orthogonal units required; torque varies with orientation	-
Disturbance Rejection	Low/Medium	Effective for slow, small disturbances; poor for high-torque events	[15]
Precision Pointing	Low	Insufficient for sub-arcsecond alignment (Low Torque)	-
Mass & Volume	Low	30g/cm length	[15]
Power Consumption	Low	$\approx 1W$	[15]
Reliability	High	No moving parts; minimal failure modes	[14]
Saturation Risk	N/A	N/A—does not accumulate momentum but cannot desaturate itself	[14]
Integration Simplicity	High	Simple electrical interface	[15]
Thermal Capability	High	Operates reliably from –20 °C to +60 °C	[15]

Table 6: Magnetorquer performance vs. mission criteria

2.3.4 Control Moment Gyros

Control Moment Gyros (CMGs) utilise high-speed rotors mounted on gimbals to generate torque through gyroscopic coupling [16] By controlling the gimbal rate Ω_{gimbal} the CMG produces torque

$$\mathbf{T}_{\text{CMG}} = \mathbf{\Omega}_{\text{gimbal}} \times \mathbf{H}_{\text{rotor}} \tag{3}$$

Where H_{rotor} is the rotor's angular momentum [17]. CMGs deliver very high torque often tens of N.m per CMG allowing fast rapid reactions and very reliable disturbance rejection, thus making them a viable solution for time-dependant tasks during repair [16].

However, CMGs introduce a huge amount of mechanical complexity and mass all while requiring more sophisticated algorithms to stabilise attitude [17]. In addition to this, the continuous actuation causes a higher average power draw relative to other actuator types. In addition, integrating CMGs is a difficult task since a vast amount of redundancy is needed due to the high risk of failure due to the complex design [18].

Table 7 summarises the performance of CMGs against the mission-specific selection criteria:

Criterion	**Rating**	**Key Note**	**Ref.**
Torque	Very High	Up to 75 N·m per CMG	[19]
Three-Axis Control	High	Different configurations offer control with redundancy	-
Disturbance Rejection	High	Fast torque response ideal for handling large disturbances	[16]
Precision Pointing	High	Sub-arcsecond pointing achievable with appropriate control algorithms	[16]
Mass & Volume	High	Typical weight $\approx$ 28kg	[16]
Power Consumption	Medium	Max 95 Watts	[19]
Reliability	Medium	Gimbal wear and motor failure risk; requires redundancy	[17]
Saturation Risk	Low	Large momentum storage capacity	-
Integration Simplicity	Low	Complex mechanical and software integration; structure must support torque loads	[16]
Thermal Capability	High	Operates between –20 °C and +60 °C	[19]

Table 7: Control-Moment Gyro (CMG) performance vs. mission criteria

2.3.5 Actuator Alternative Analysis

In order to identify the actuator that best suits the repair satellite mission, each one was evaluated in a trade-off analysis against the predefined selection criteria.

Table 8 summarises the results of the risk analysis;

Criterion	Reaction Wheels	Micro-Thrusters	Magnetorquers	Control Moment Gyros
Torque	High	High	Low	Very High
Three-Axis Control	High	High	Medium	High
Disturbance Resistance	Medium/High	Medium/High	Low/Medium	High
Precision Pointing	Very High	Medium	Very High	Low
Mass & Volume	Medium	Medium	Low	Medium
Power Demand	Medium	Low	High	Low
Reliability	High	Medium	Medium	High
Saturation Risk	High	Medium	Low	High
Integration Simplicity	High	Medium	Low	High
Thermal Compatibility	High	High	Medium	High
Orbit Suitability	High	High	Medium	Medium

Table 8: Trade-Off Analysis of Candidate Attitude Actuators

Based on the comparative trade-off analysis, the actuator configuration can be chosen.

The combination of four RWs with micro-thrusters for desaturation was selected as the optimal SACS solution for the repair mission. As discussed, RWs provide very high precision pointing, with loss mass relative to performance but with very high reliability thus, making them perfectly suited for the fine control and rigorous stability requirements during the in-orbit repair. However, due to the high risk of saturation, especially in the presence of large disturbances (such as possible ones caused by the arm) micro-thrusters have been chosen to be incorporated to desaturate the RWs and unload angular momentum efficiently.

The hybrid approach selected, provides good trade-off and balance between torque, precision,reliability,redundancy and system integration complexity.

CMGs, whilst offering a higher torque than the selected configuration, they introduce significant challenges with mechanical and computational complexity, mass and failure risk. Magnetorquers, whilst reliable, simply lack the torque needed for the repair mission. Therefore, the 4RW + micro-thruster offers the most robust, mission appropriate solution.

2.4 Sensor Design Alternatives

2.4.1 Sensor Alternatives

Following the selection of the actuator configuration, it's imperative to define a complementary array of sensors such that the SACS is provided with accurate and continuous attitude and angular rate information. The performance of the actuator configuration is dependant on the sensor performance .

Table 9 details the key sensor technologies considered for the repair mission, showing their functions, advantages and limitations.

Sensor Type	**Use Case**	**Key Notes**	**Ref.**
Sun Sensor	Attitude Measuring	Low mass, low power but not functional during eclipse; accuracy ≈0.5°	[17, 20]
Magnetometer	Attitude measuring using field sensing	Passive, robust in LEO; EMI-sensitive.	[17]
Star Tracker	Primary attitude reference	High accuracy (; sensitive to sunlight; high cost	[17]
Gyroscopes	Angular rate tracking	Enables real-time measurements; suffers from drift	[17]
Earth Horizon Sensor	Nadir-pointing	works only in LEO	[21]

Table 9: Sensor Design Alternatives for Attitude Determination

These are then assessed not just in the individual performance but also how they will integrate with the actuator configuration and performance on it section is weighted (from Very High to Low see Table 10)

Criteria	**Sun**	**Magnet**	**Star Tracker**	**Gyroscope**	**Earth Sensor**
Mass	High	High	Medium	Low	Medium
Power Consumption	High	High	Low	Low	Medium
Accuracy	Low	Low	High	High	Medium
Complexity	High	High	Low	Medium	Medium
Cost	High	High	Low	Medium	Medium
Update Rate	High	High	Medium	High	Medium
Environmental Dependence	High	Medium	Low	Low	High
Autonomy	Low	Low	High	High	Medium

Table 10: Comparison of attitude sensors across key criteria (High = Good)

2.4.2 Sensor Alternatives Analysis

In order to support the actuator choice and high precision of the SACS needed for the repair mission, a sensor combination of a sun tracker and gyroscope has been selected. The sun tracker will serve as the primary attitude reference, providing the orientation with very high accuracy [17] which is necessary for maintaining the stable performance of the SACS for a wide range of disturbances. In addition to this, the gyroscope, will offer quick angular velocity measurements. The combination of the two allow for the high precision and robustness needed for the in-orbit repair.

In contrast, Earth sensors are limited greatly by environmental conditions as line of sight is often obscured and in terms of during the repair, attitude must be very stable. On the other hand, magnetometers suffer from poor accuracy when away from Earths magnetic field.

2.5 Design Specifications And Regulations

2.5.1 Design Regulations And Standards

Following the selection of the actuator and sensor configuration, it's essential to evaluate the regulatory implications of the system design leading to the final design specifications. Both the actuators and sensors are subject to standards governing EMI, safety and debris mitigation. Table 11 outlines the key regulatory constraints that directly impact the final design specifications that the final design must comply with in order to integrate with the wider space environment.

Constraint	**Description**
Space Debris Mitigation	Compliance with debris generation; 25-year deorbit rule.
Proximity Licensing	National regulatory authorization required for rendezvous and repair missions.
EMC Compliance	standard for internal electromagnetic compatibility.
Liability	Launching state assumes liability under the Outer Space Treaty; insurance may be required.

Table 11: Summary of Regulatory Constraints for Satellite Servicing

2.5.2 Design specifications

With the actuator configuration and sensors defined, numerical design specifications can be constructed with feasible goals for the SACS

Constraint	Value / Range	Reason / Impact
Pointing Accuracy	1°	Critical for stability.
Torque (Max Reaction Wheel)	±0.02 Nm	Sets the maximum control.
Response Time	$< 75s$	Indicates how quickly the SACS stabilises.
Peak Power Consumption	70W	Limits load on power subsystem (and thermal design).
Mass of SACS	10 kg	Essential for meeting overall satellite mass constraints.
Alignment Tolerance (RWs)	2° misalignment	Misalignment reduces control efficiency .
Thruster Switching Time	0.1 s	Affects timing precision during momentum dumping and fast control responses.

Table 12: Physical constraints for a 4-Reaction Wheel and Thruster Attitude Control System

3 Technical Description Of Attitude Control System

The final SACS was implemented using MATLAB/SIMULINK in order to rigorously test, simulate and validate system performance under a wide array of conditions. The Simulink model was structured with clear blocks showing how every component was used and implemented in the control system in order to achieve a reliable and robust end result.

3.1 Block Diagram Overview

Figure 9 details the high level block diagram of the final SACS design with clear labelled subsystem blocks ans signals (in red) [22].

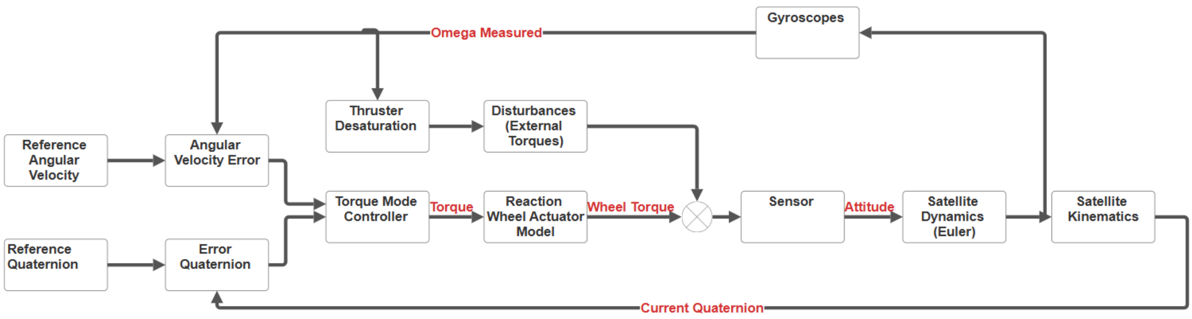

Figure 9: High-Level Block Diagram of SACS

The key functions and subsystems for the SACS design are

- **Reaction Wheels Subsystem:** Implements torque generation through reaction wheels.
- **Thruster Subsystem:** momentum desaturation, enabling sustained operation without loss in performance.
- **Gyroscope and Sun Sensor Inputs:** Provide real-time orientation feedback crucial for real-time closed-loop attitude control.
- **Quaternion Computation Module:** Converts sensor feedback into quaternion for mathematical processing.
- **Torque Controller Logic (PID/PD Block):** Adjusts error signals to command signals for the RWs.

3.2 Quaternion Mathematics and Controller Implementation Methodology

The SACS makes use of quaternion mathematics to represent the satellites rotation and orientation, to allow for simple mathematical processing and reference modelling all while providing numerical stability that cannot be achieved in specific events due to Euler angle representation[22, 23, 24].

3.2.1 Quaternion Theory

Quaternions are essentially a four-dimensional vector expressed as such [23]:

$$q = \begin{bmatrix} q_1 & q_2 & q_3 & q_4 \end{bmatrix}^T \tag{4}$$

Where q_4 is the scalar component, and q_1,q_2,q_3 are the orientation about the x ,y and z axes respectively [24]. The control system throughout the operation continuously computes the error(q_e) between a desired quaternion and a feedback quaternion (which represents the current orientation of the satellite). This is calculated using equation 5 [25, 24].

$$q_e = q_d \otimes q_f^* \tag{5}$$

Where q_d is the desired quaternion and q_f is the feedback quaternion. The result of this equation is then subsequently an input into a tuned PD controller used to generate the torque command signal to the RW actuators.

3.2.2 Quaternion Simulink Implementation

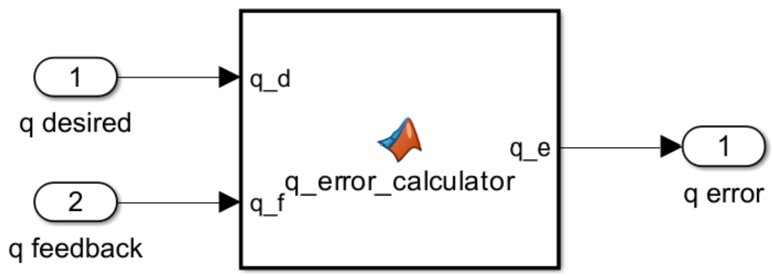

Figure 10: Simulink Model Of Quaternion Error Calculator

The quaternion error Calculator (Figure 10) implements equation 5 in a MATLAB function taking the 4x1 vector inputs of the desired quaternion (q desired) and the current quaternion of the system (q feedback) and outputs the error (To be used in controller).

The function as shown in Listing 1 details the exact function. No pre-made function has been used and the conjugate and and inverse were manually coded using matrix theory.

Listing 1: Quaternion Error Calculator Function

```
%Made By DRS46
%Function that inputs desired quaternion (from wanted attitude) and
%calculates the error based on the current quaternion of the SACS

%All in standard form [x, y, z, w] where w is the scalar component

function q_e = q_error_calculator(q_d,q_f)

%Extracts x,y,z and scalar components
x = q_d(1);
y = q_d(2);
z = q_d(3);
scalar = q_d(4);

%Calculates the conjugate quaternion of q feedback
q_c = [-q_f(1); -q_f(2); -q_f(3); q_f(4)];

%Builds the 4x4 multiplication matrix for q desired
Q_d = zeros(4,4);
Q_d(1,:) = [ scalar,  z, -y,  x];
Q_d(2,:) = [-z,  scalar,  x,  y];
Q_d(3,:) = [ y, -x,  scalar,  z];
Q_d(4,:) = [-x, -y, -z,  scalar];

%Computes the error quaternion with a 0.5 scalar component to allow for
%simulation efficiency
q_e = 0.5 * Q_d * q_c;

end
```

3.2.3 Quaternion Error Proof Of Concept

3.2.4 Torque Mode Controller Mathematics

The torque controller plays an integral and efficient part of the SACS. It has inputs of the current value of the angular velocity and current quaternion (measured from sensors) and outputs the command torque signal for the RW actuator system.

Due to the three-axis nature of the system, The output from the controller should be relevant to the x,y and z axis. Equation 6 [23] details the mathematical formulation the controller implements

$$\tau_c = -K_p \cdot \begin{bmatrix} q_{e1} \\ q_{e2} \\ q_{e3} \end{bmatrix} - K_d \cdot \begin{bmatrix} \omega_{x,e} \\ \omega_{y,e} \\ \omega_{z,e} \end{bmatrix} \tag{6}$$

where τ_c is the command torque (3x1 vector) , K_p is the proportional gain, K_d is the differential gain and w is the angular velocity error in either the x,y or z plane. A PD controller was used instead of a PID as a deliberate engineering trade-off since PDs are simpler to tune and implement whilst offering fast response and good stability for rotational dynamics and the integral term (I) aids in eliminating steady state error (but in this case transient response is much more important) [26, 24].

3.2.5 Torque Controller Simulink Implementation

The torque mode controller was implemented and tuned in Simulink as seen in Figure 11:

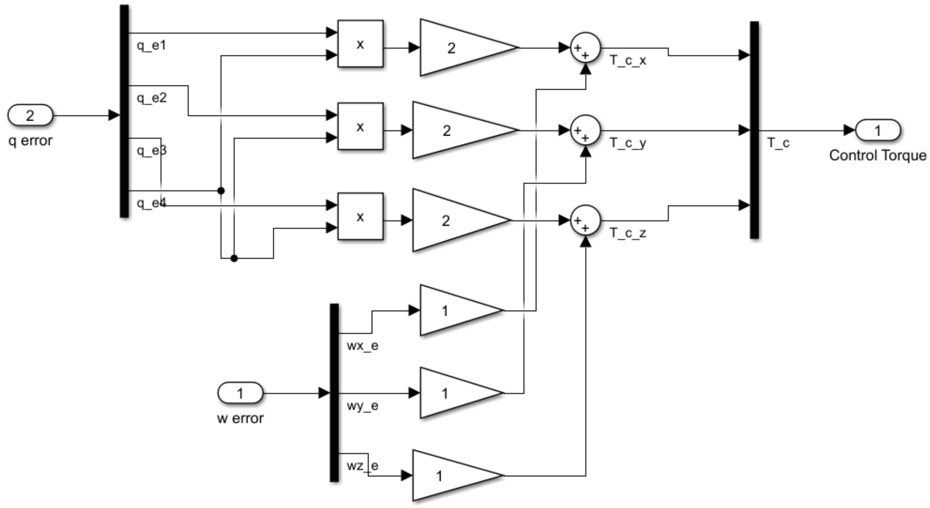

Figure 11: Simulink Model Of Torque Controller

The proportional gain controls the response to the orientation error, while the derivation gain will dampen rapid oscillations [26]. Both gains were tuned through simulation to meet the pointing accuracy and stability requirements. (in this case $K_p = 2$ and $K_d = 1$). The output control torque is a 3x1 vector of torque values relevant to the axis

The angular velocity error was implemented by very simply subtracting the reference from the feedback value (Figure 12).

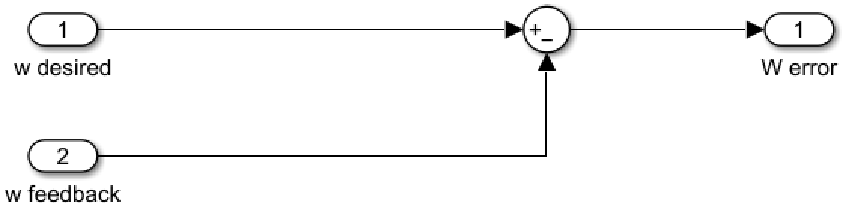

Figure 12: Simulink Model Of Angular Velocity Error

3.3 Actuator Subsystem

The actuator model is essential in converting the control torque computed by the controller and distributing it efficiently to the RWs to allow for maximum stability.

3.3.1 Reaction Wheel Configuration

A pyramidal configuration is employed, where the four RWs are mounted at equal angles relative to each other thus enabling omnidirectional torque generated throughout the three axes of movement. This layout provides full three degrees of freedom with the fourth wheel providing redundancy in case of a single event failure. In addition to this, the layout ensures that no wheels are located where it is able to provide torque on just one axis [24]. (See Figure 13)

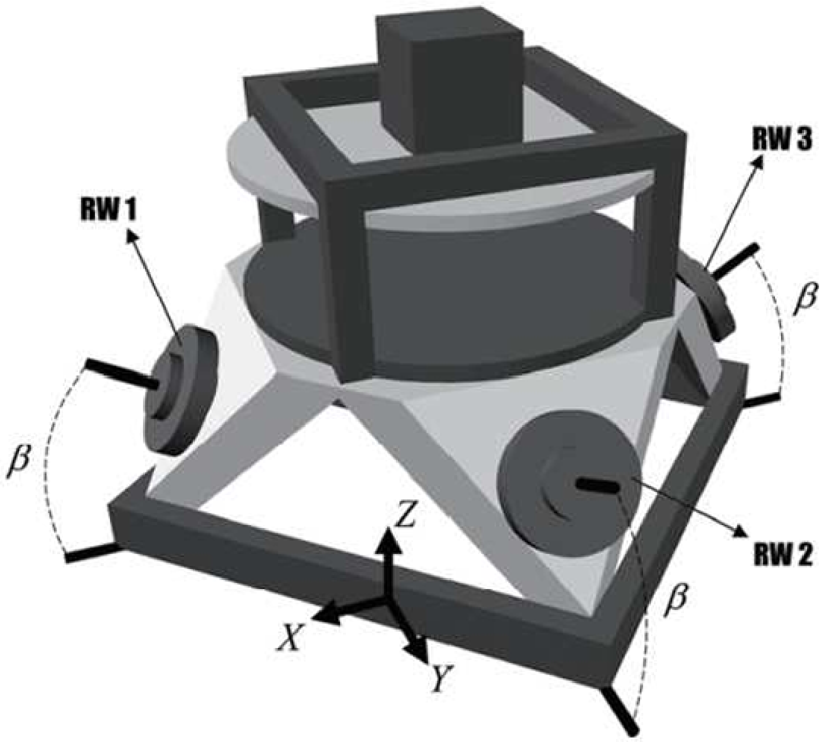

Figure 13: Pyramid RW Model [24]

From this, the RWs tilt-angle (β) can be chosen in a way that maximises goals such as power consumption, fewest error and reaction time [24].

The torque from the wheels can be defined as such [24]:

$$\begin{bmatrix} T_{C_x} \\ T_{C_y} \\ T_{C_z} \end{bmatrix} = \begin{bmatrix} \cos\beta & 0 & -\cos\beta & 0 \\ 0 & \cos\beta & 0 & -\cos\beta \\ \sin\beta & \sin\beta & \sin\beta & \sin\beta \end{bmatrix} \begin{bmatrix} T_1 \\ T_2 \\ T_3 \\ T_4 \end{bmatrix} \tag{7}$$

where T_c is the control torque , $\cos\beta$ is in the x direction, $-\cos\beta$ is in the y and T_N is the wheel torque thus, the wheel torque can be calculated as such:

$$T_N = A^* T_C \tag{8}$$

where A^* is the pseudo inverse of the coefficient matrix.

3.3.2 Simulink Model And Implementation

In the Simulink model derived for the SACS it is imperative that the angle β is optimisable and not a fixed value (as referred to in equation 7). Figure 14 details, the implementation of the individual wheels (where each wheel is a column of equation 7)

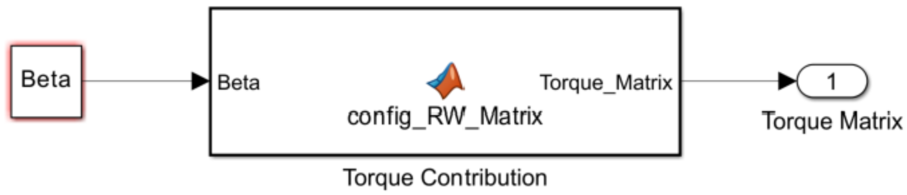

Figure 14: Single RW Model

Where Beta is the angle as seen in Figure 13.

Listing 2: Individual Torque Combination Of A Wheel

```
function Torque_Matrix= config_RW_Matrix(Beta)
%MADE BY DRS46

%INDIVIDUAL TORQUE CONTRIBUTION OF MATRIX
Torque_Matrix = [cos(Beta);0;sin(Beta)];

end
```

Listing 2 details how the matrix formulated in equation 7 has been decomposed into individual torque contributions. Specifically noting how all components contribute to the z axis but only individually to the x or y plane.

Equation 7 is then fully implemented as seen in Figure 15:

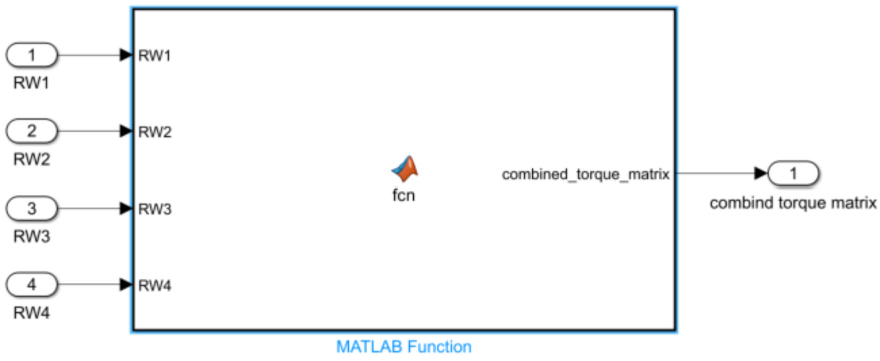

Figure 15: Combined matrix model

The function simply combines the torque contributions to formulate fully equation 7 (See Listing 3).

Listing 3: Individual Torque Combination Of A Wheel

```
function Torque_Matrix= config_RW_Matrix(alpha)
%MADE BY DRS46

%INDIVIDUAL TORQUE CONTRIBUTION OF MATRIX
Torque_Matrix = [cos(alpha);0;sin(alpha)];

end
```

The final necessary step as discussed is to create the wheel torques from the body torques (see equation 8) as is implemented in the MATLAB function in Listing 4.

Listing 4: Pseudo Inverse Matrix

```
function Combined_torque_matrix_pinv = torque_pinv_matrix(Combined_torque_matrix)

%CREATED BY DRS46
%Creates the pseudo-inverse matrix which then maps wheel torques to body
%torques
Combined_torque_matrix_pinv = pinv(Combined_torque_matrix);
```

This function is implemented in the wider design as detailed in Figure 16:

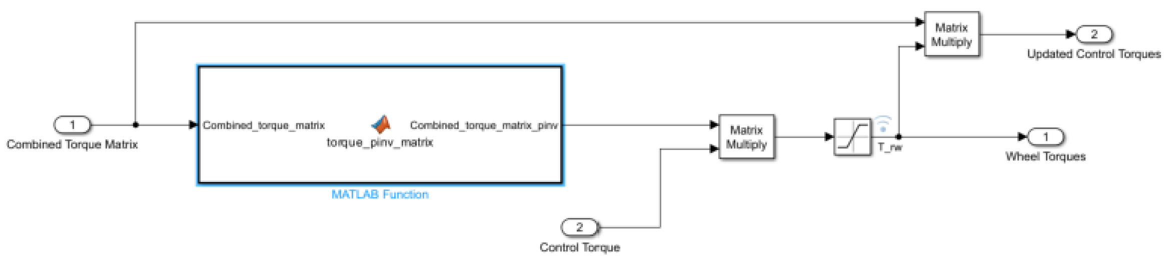

Figure 16: Pseudo Inverse Combined matrix model

This is a crucial element in the RW model in terms of torque application , Here, after the body and control torques have been mapped to the wheels through matrix multiplication, they are saturated at a value as per the design specification (0.02 Nm) and the chosen real world reaction wheel that could be implemented . The saturation value is also implemented to update control torques with this saturation level (which is to be implemented in the dynamics [24]).

Figure 17 details how all these RW sections combine to form the full actuator model with 4 RWs:

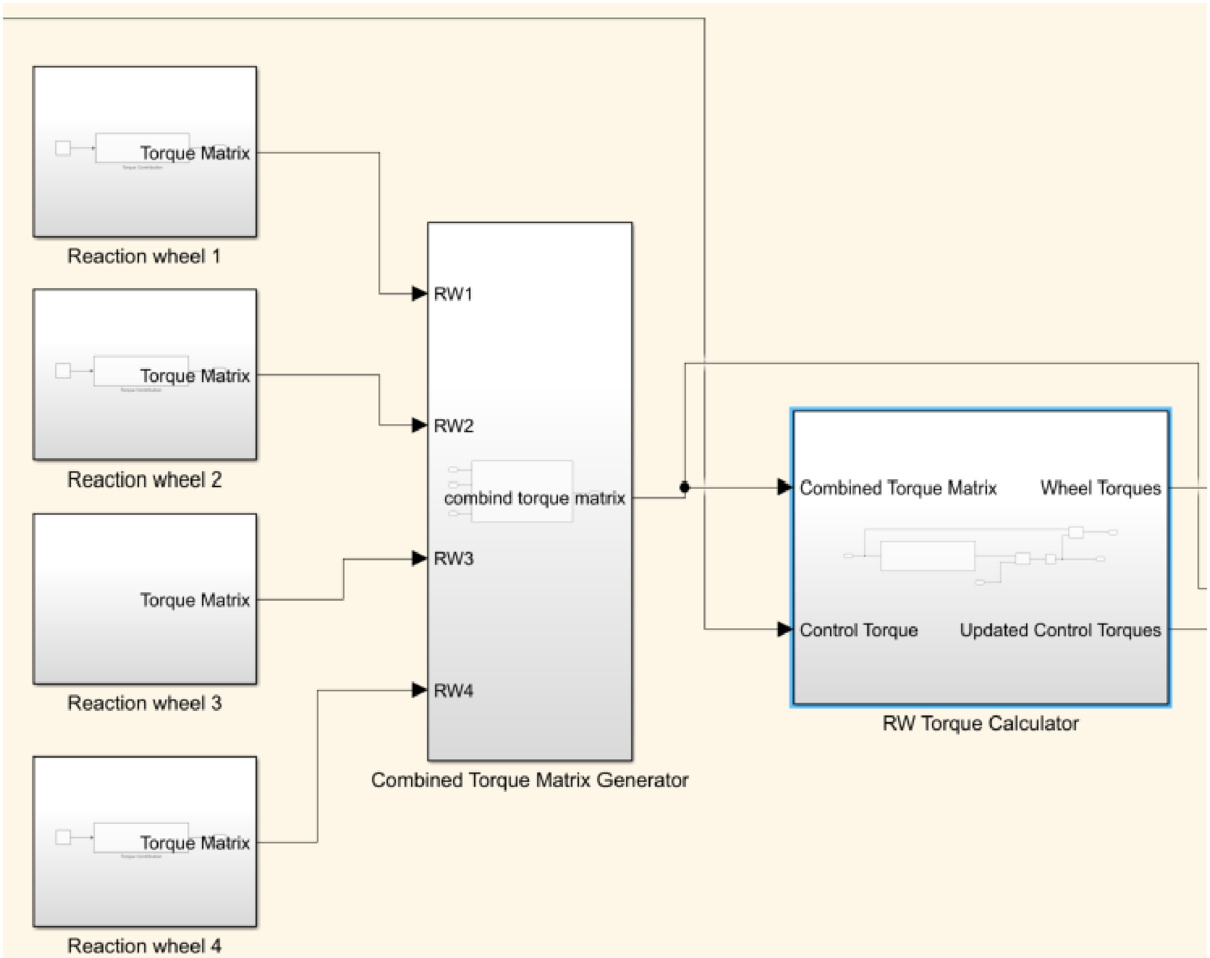

Figure 17: Completed Four RW model

3.3.3 RW Selection

3.4 Thruster Subsystem

The thrusters must apply a brief, controlled pulse of force opposite to the direction of accumulated momentum.

3.4.1 Thruster Configuration Design

A configuration of four Micro cold-gas thrusters has been adopted, when positioned orthogonally about the satellite's body axes will proved full three-axis control with redundancy [11].

The exact thruster layout is more akin to the satellite platform design as thrusters will have to be placed in a manner such that sensitive equipment aren't interfered with during the burn process.

3.4.2 Thruster Controller Mathematics

The thrusters are to be controlled with a Pulse-Width Pulse-Frequency Modulation controller (PWPF). (Figure 18)A controller where the actuator is either fully on or off thus saving on fuel , power all while smoothing actuation [22].

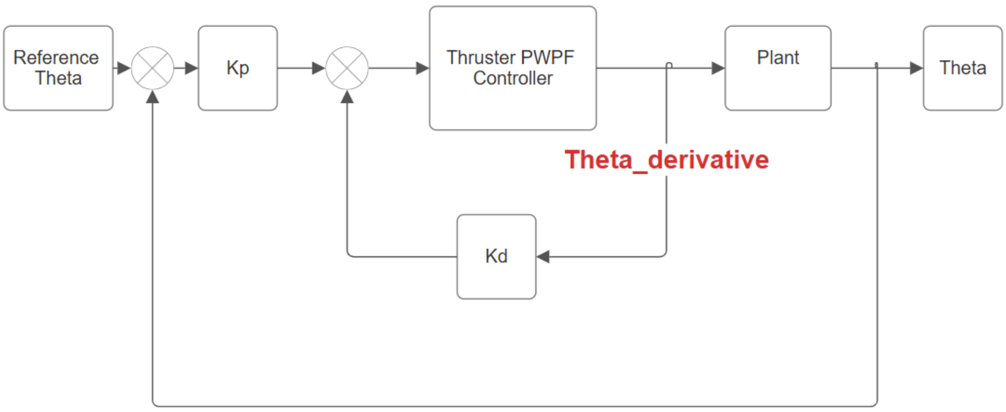

Figure 18: Thruster Overview Block Diagram

The decision was made to implement the thruster control using a binary on/off controller for a magnitude of reasons;

- **Simplicity:** Simple logic and is very robust with few moving parts and sensors [27].
- **Precision:** Simulates analog behaviour by modulating the pulse width (time on) and pulse frequency (how often they are triggered) thus achieving a smooth control over time [27, 28].
- **Fuel Efficiency:** Avoids continuous fuel burns thus improving efficiency and consequently lifespan of the SACS [28] .

A PWPF controller consists of a first order filter and a Schmitt trigger (in a feedback loop) [22].

3.4.3 Simulink Model And Implementation

Figure 19 details the first-order filter equation used to smooth rapid changes and shapes the control input prior to triggering [22].

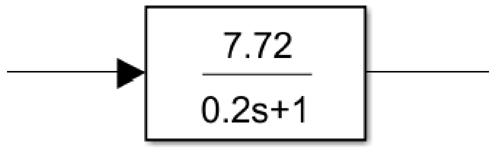

Figure 19: Filter For PWPF

The filtered signal must then be fed to a Schmitt trigger to generate an On/Off output (Listing 5).

Listing 5: Bipolar Schmitt Trigger

```
%Function For Bipolar Trigger In Simulink

function output = schmitt_trigger_bipolar(input)
%CREATED BY DRS46

%Trigger has values (U_on) that are where it triggers and H_pos
    which is
%values for binary 1

    Uon_pos = 0.45;
    Uon_neg = -0.45;
    H_pos = 0.3;
    H_neg = -0.3;
    output = 0; %Value if not high or low

    if input >= Uon_pos
        output = H_pos;

    elseif input <= Uon_neg
        output = H_neg;

    elseif input > Uon_neg && input <Uon_pos
        output = 0;
    end
```

For an continuous torque control input, the trigger operates as detailed in Figure 20.

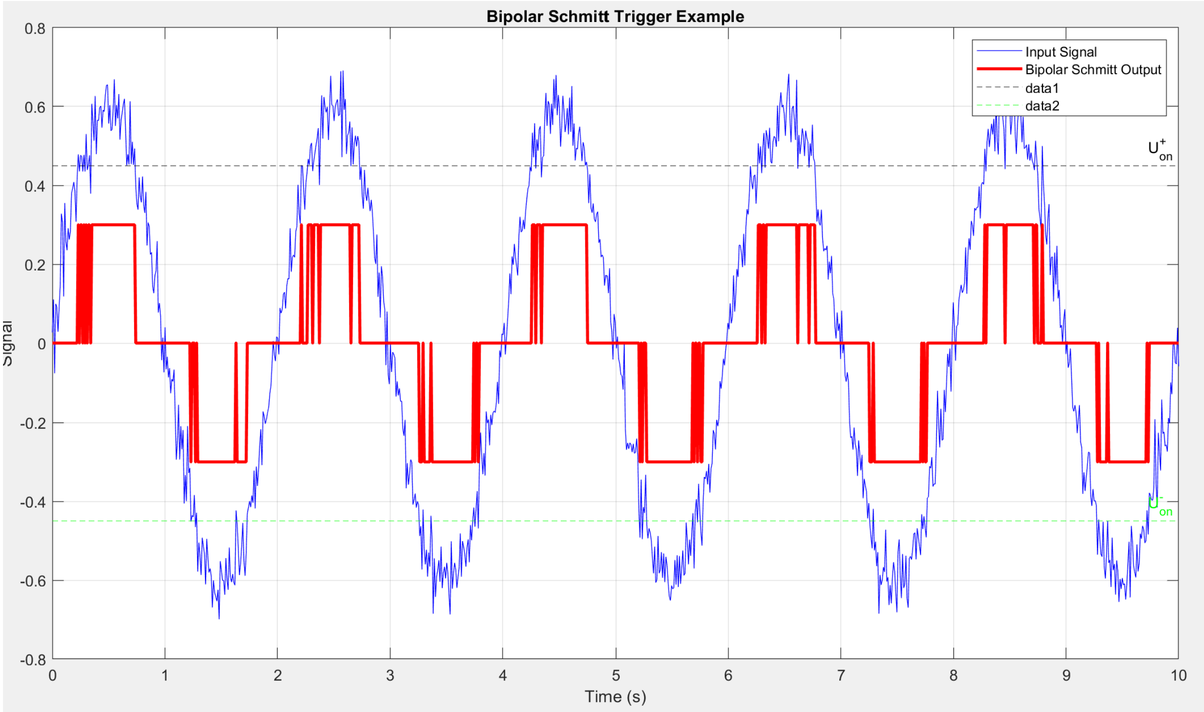

Figure 20: Schmitt Trigger Functionality

Thus from this design, the thrusters will burn on an ON/OFF methodology based on the error between the output and the reference angular rate until desaturation is achieved.

The fully realised system is detailed in Figure 21:

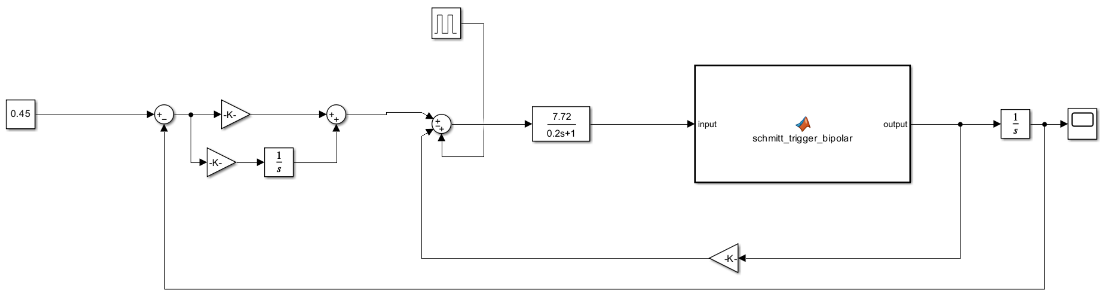

Figure 21: Completed Simulink Model For Thruster Control

3.5 Environmental And Arm Disturbances

3.5.1 Modelling Approach

A technical component needed to test for the validity of the SACS in terms of the in-orbit repair mission is to effectively simulate how the SACS operates in the presence of external torques caused by two key areas:

- **Environmental:** External pressures and torques caused by the space environment.

- **Arm:** Torques generated as a result of the repair process taking place.

Modelling these disturbances in both worst case and best case scenarios is imperative for functional testing.

3.5.2 Environmental Disturbances

Environmental torques were modelled assessing the SACS performance under intrinsic low amplitude but constant forces:

- **Gravity Gradient Torque:** Modelled by $\tau_{gg} = 3\mu(r)^{-3}(I_z - I_y)\sin 2\theta$ [29].
- **Solar Radiation Pressure:** Continuous but dependant on surface area and angle of incident [30].
- **Magnetic Torque:** $\vec{T} = \vec{M}_{\text{dipole}} \times \vec{B}$ [15]
- **Aerodynamic Torque:** Only included in altitudes ¡ 500km.

Each was integrated into a MATLAB configurable function to be utilised in the SACS Simulink (Listing 6).

Listing 6: Bipolar Schmitt Trigger

```
function tau_env = environmental_torques(t)
% ENVIRONMENTAL_TORQUES
% Solar Radiation Pressure (Here we are assuming a value and
    constantly operating around the x axis)
tau_srp = 0.0015;  % Nm
% Gravity Gradient Torque: (As per the equation it is a
    sinusodial function around the y axis)
tau_gg = 0.0035 + 0.0015 * sin(0.1 * t);  % Nm
% Magnetic Torque (Sinusodial and varying around the z axis)
tau_mag = 0.0005 + 0.0003 * sin(0.3 * t + 1);  % Nm
% Aerodynamic Torque (Very Very small)
tau_aero = 0.0002 + 0.0001 * sin(0.2 * t + 2);  % Nm
%Summed around x,y and z plane
tau_env = zeros(3,1);
tau_env(1) = tau_srp;
tau_env(2) = tau_gg + tau_aero;
tau_env(3) = tau_mag;
%tau_env is complete 3 axis form of environmental torque
end
```

Leading to torque over time as seen in Figure 22:

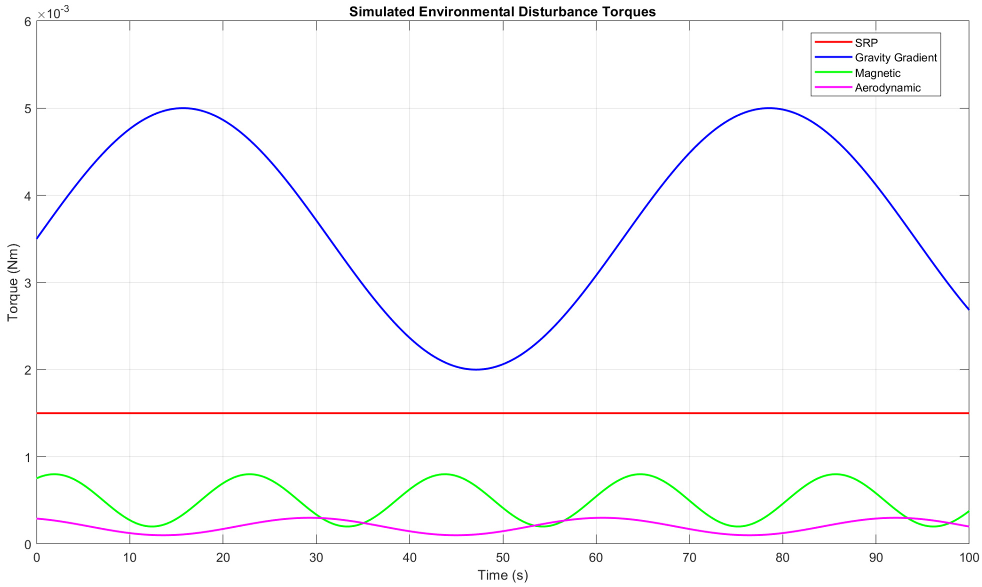

Figure 22: Environmental Torque Vs Time

3.5.3 Arm Disturbances

As a consequence of the repair mission relatively large disturbances will be acting upon the satellite that the SACS must react to. The torques were modelled using the rigid body dynamics equation [17]:

$$\boldsymbol{\tau}_d = \mathbf{I}_a \cdot \dot{\boldsymbol{\omega}}_a + \boldsymbol{\omega}_a \times (\mathbf{I}_a \cdot \boldsymbol{\omega}_a) \tag{9}$$

This is known as the Euler equation of rotational motion of a rigid body (An arm in this case) [17]. The first term $\mathbf{I}_a \cdot \dot{\boldsymbol{\omega}}_a$ is the torques from angular acceleration and the second term is the gyroscopic torque.

This was implemented in a MATLAB function (Listing 7) that approximates the torques seen throughout a repair mission with points in time of high disturbances and points of low disturbances.

Listing 7: Arm Disturbance Mission Estimation

```
function tau_arm = arm_disturbance_torque(t)
%PLAN FOR THE MISSION EXAMPLE
% t = 0  10s  : idle
% t = 10  30s  : Arm Start Moving (medium to Low torque)
% t = 30  50s  : fast Moving (high torque As Arm move)
% t = 50  70s  : hold (small Torque as Repair takes place)
% t = 70  100s  : retract (moderate torque As arm is retracted and repair is completed)
tau_arm = zeros(3,1); %Creates 3-axes out
%Mission parameter from 0 to 10s
```

```
if t >= 10 && t < 30
    tau_arm(1) = 0.02 * sin(0.5 * t); % Nm in X
    tau_arm(2) = 0.015 * sin(0.6 * t); % Nm in Y
    tau_arm(3) = 0.01 * sin(0.4 * t);  % Nm in Z
%Mission parameter from 30 to 50s
elseif t >= 30 && t < 50
    tau_arm(1) = 0.05 * sin(0.7 * t);
    tau_arm(2) = 0.04 * sin(0.8 * t + 0.5);
    tau_arm(3) = 0.03 * sin(0.6 * t + 1);
%Mission parameter from 50 to 70s
elseif t >= 50 && t < 70
    tau_arm(1) = 0.005 * sin(0.3 * t);
    tau_arm(2) = 0.005 * sin(0.3 * t);
    tau_arm(3) = 0.005 * sin(0.3 * t);
%Mission parameter from 70 to 100s
elseif t >= 70 && t <= 100
    tau_arm(1) = 0.02 * sin(0.5 * t + 1);
    tau_arm(2) = 0.015 * sin(0.6 * t);
    tau_arm(3) = 0.01 * sin(0.4 * t + 0.5);
end
end
```

Where Equation 9 relates as shown in Table 13.

Component	**Implementation In Code**
$\dot{\omega}_a$	Angular acceleration implemented via the frequency and amplitude of the sinusoidal wave.
ω_a	Angular velocity implemented through the shape of the output.
$\mathbf{I}_a$	Scaling Component of the function.
$\boldsymbol{\tau}_d$	Output disturbance torque vector.

Table 13: Comparison Between Rigid Body Torque Model and Code Approximation for Robotic Arm Disturbance

This will provide a disturbance torque profile over time as expected on a repair mission (See Figure 23)

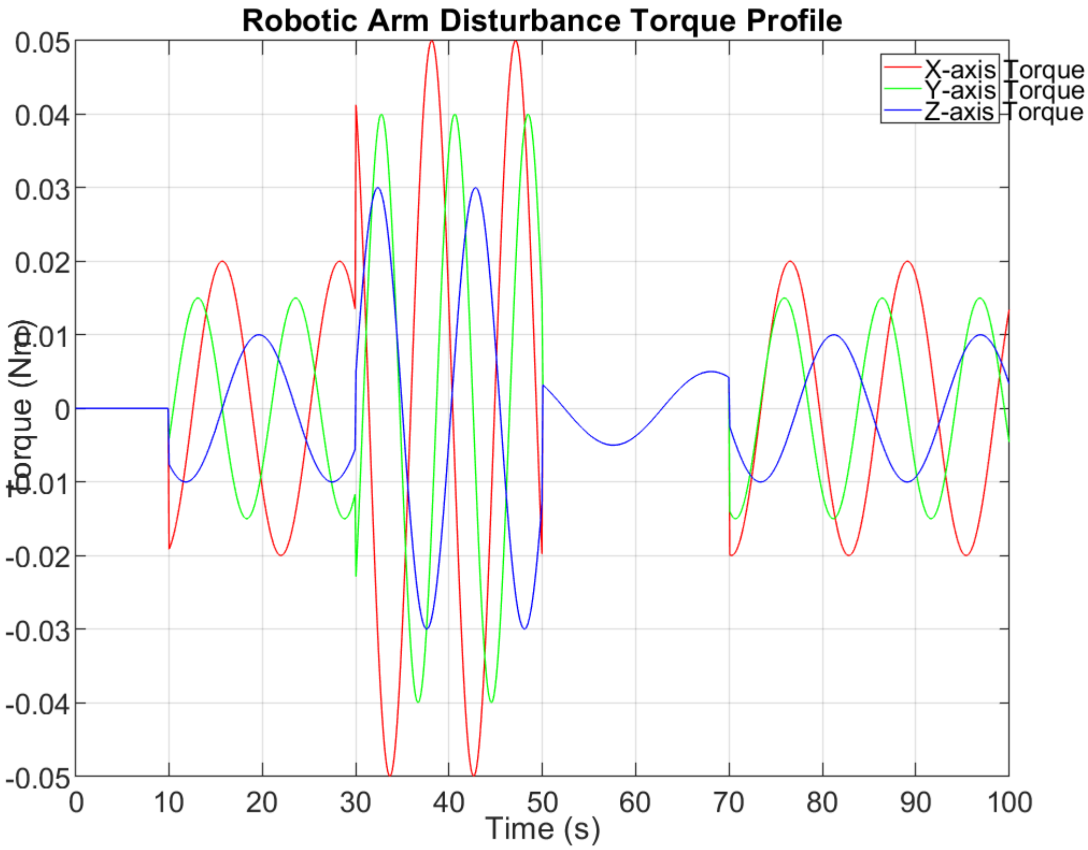

Figure 23: Graph For Arm Disturbance

3.6 Kinematics And Attitude Dynamics

3.6.1 Mathematical Basis

The satellites rotational dynamics are likewise implemented using equation 9. But includes the body moment of Inertia in order to compute angular acceleration from the applied wheel torque [24].

The dynamics module essentially is calculating the reaction wheels speed over time based on all the inputs and internal dynamics of the satellite and actuators [24].

The satellite kinematics utilises quaternion mathematics to calculate the current quaternion from the angular velocity of the RWs utilising the equation:

$$\dot{\mathbf{q}} = \frac{1}{2}\,\Omega(\boldsymbol{\omega})\,\mathbf{q} \tag{10}$$

Where $\Omega(\boldsymbol{\omega})$ is the screw matrix [24].

3.6.2 Simulink Implementation

The Satellite Dynamics are implemented as detailed in Figure 24:

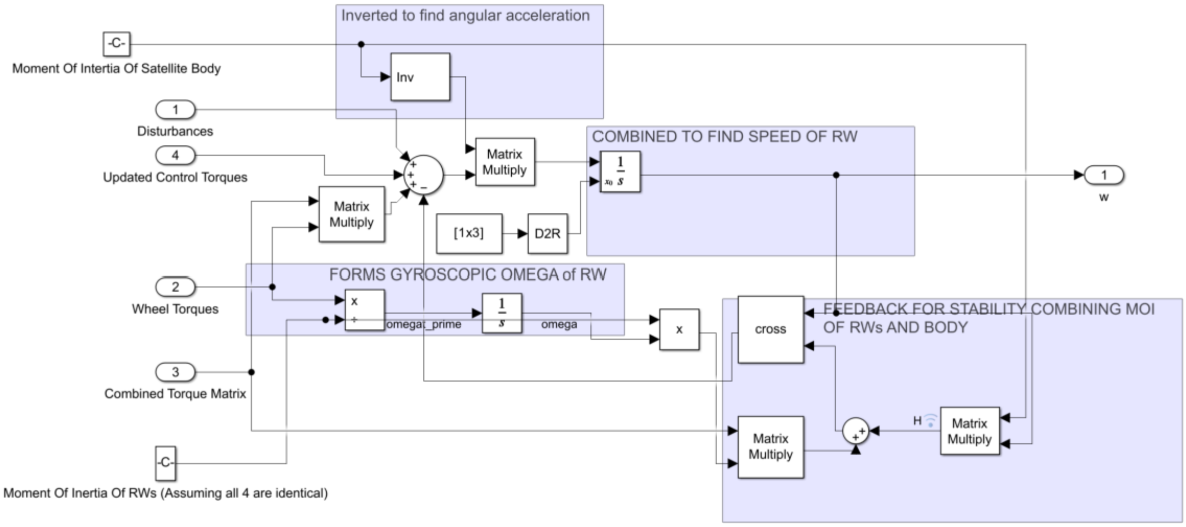

Figure 24: Satellite Dynamics Simulink Model

The Satellite Dynamics are implemented as detailed in Figure 25:

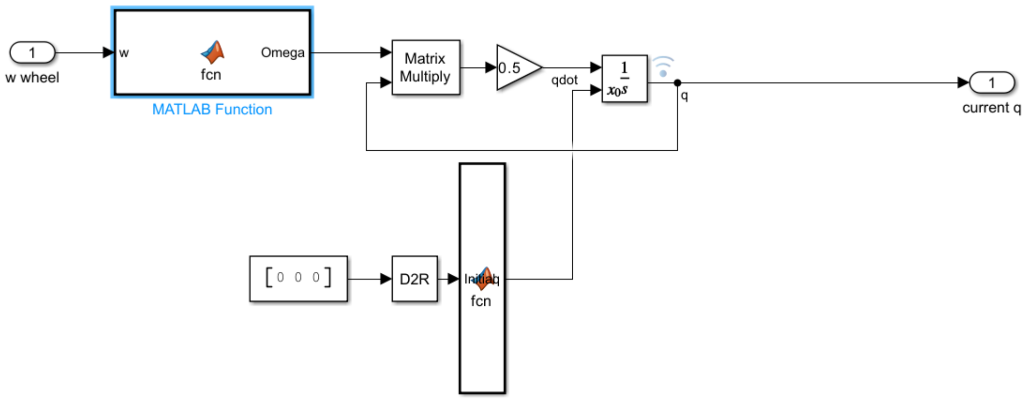

Figure 25: Satellite Kinematics Simulink Model

3.7 Final Integrated SACS Design

All of these modules and systems were integrated in order to form the full SACS that can be tested (Figure 26)

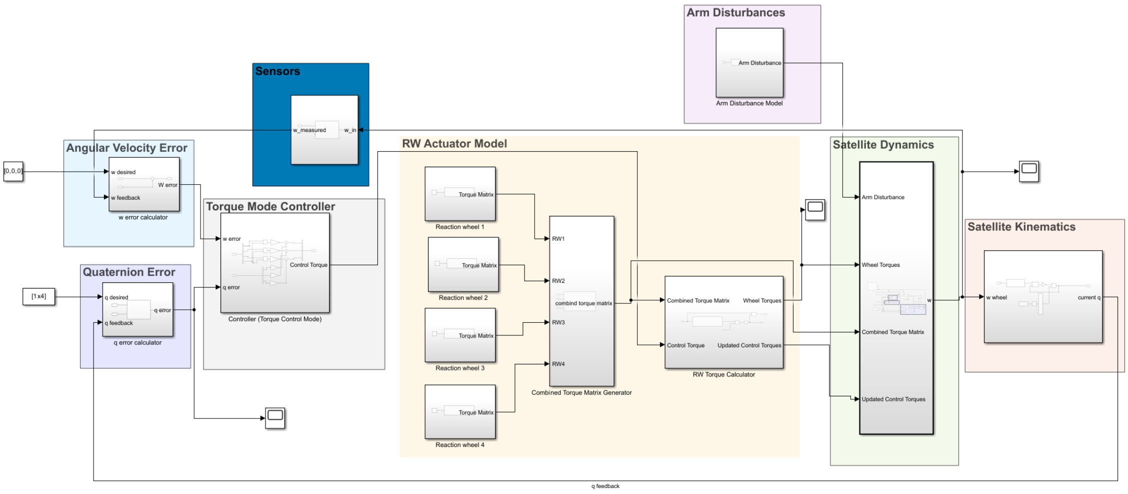

Figure 26: Fully Realised SACS

(particularly noting the sensors in the feedback path)

4 Testing Of System

4.1 Testing Plan

In order to ensure the SACS satisfies both the numerical functional and reliability requirements, a methodical test procedure was created with the Simulink system. This plan confirms

4.2 Simulink Testing And Verification

4.2.1 Ideal Conditions Operational Validation

To verify the SACS can stabilises the satellite from a range of initial orientation error, three different input conditions were tested under ideal conditions (no disturbances, no singular faults and no spin). These scenarios will assess the fine control prevision and robustness of the design.

Through rigorous testing it was found that when $\beta = 1$ radians the SACS performed the most optimally

Table 14 details the initial test scenarios and inputs:

Test	Initial Quaternion	Angular Velocity [rad/s]	Description
1	[0.01, 0.01, 0.01, 0.9998]	[0, 0, 0]	Very Small offset
2	[0, 0, 0.7071, 0.7071]	[0, 0, 0]	90° misalignment around Z-axis
3	[1, 0, 0, 0]	[0, 0, 0]	180° around X-axis

Table 14: Operational Validation Test Inputs and Initial Conditions

The three test cases in Table 14 were simulated in Simulink. For each test, the response was observed via the quaternion error, angular velocity and control torque outputs. These results provide a critical analysis of both the stability and responsiveness of the SACS.

Test 1

This tests the behaviour under a very minor attitude deviation, where the satellite is almost aligned with the target orientation, where it serves as a baseline for evaluating precision under an ideal scenario.

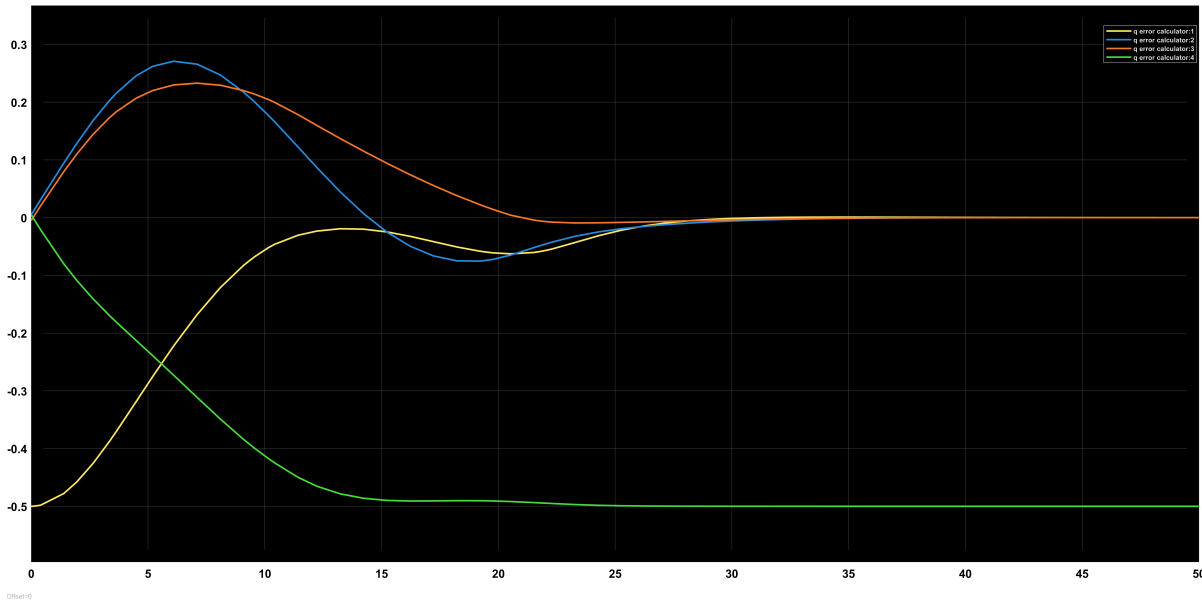

Figure 27: Quaternion Error Output - Small Deviation Test

The output over the quaternion error is seen in Figure 27, the quaternion error components q_{e1}, q_{e2}, q_{e3} start at their expected initial values (respective colours yellow,blue,red,green) and over time converge to zero, this is done within 25 seconds. Whilst, q_{e4} (the scalar component) starts at zero (i.e not aligned) and over time approaches -0.5 (in quaternions - and + are interchangeable [24]) when stability has been reached (x,y and z components are identical).

This waveform exhibits the expected output, showing the SACS responds accurately and reaches stability in a timely manner. The absence of any oscillation proves correct usage and implementation of quaternion dynamics, and Euler rotational equations to create a SACS design.

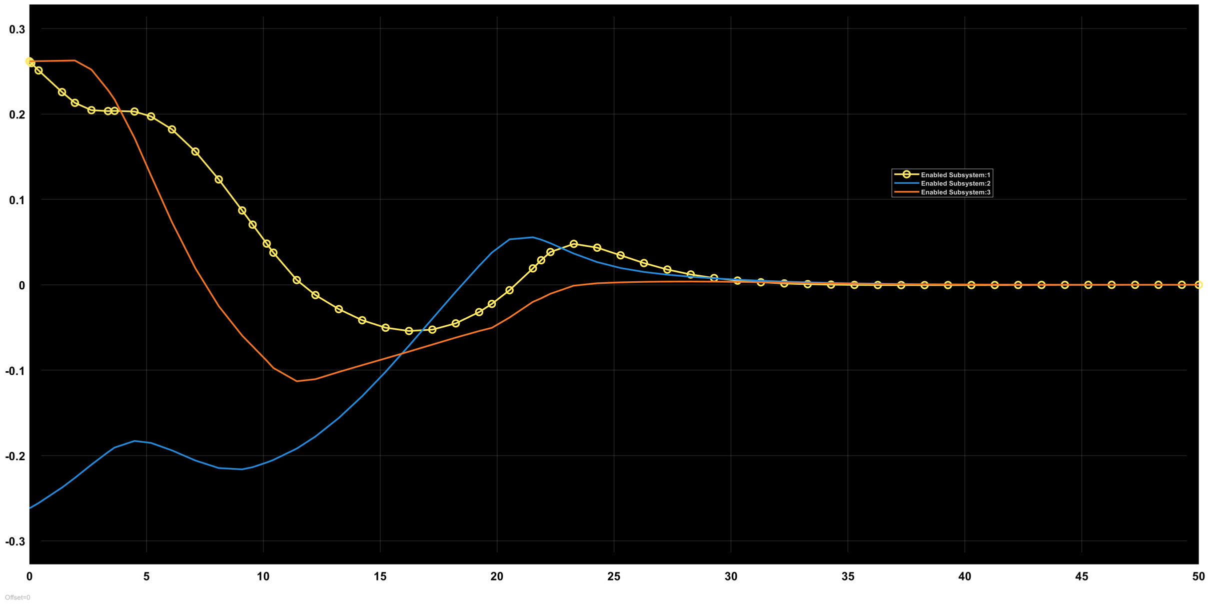

Figure 28: Reaction wheel speeds over time during small deviation test scenario.

Figure 28 shows the angular velocity response of the satellite along each of the x (yellow), y (blue) and z (red) axis. Since the satellite initially begins from rest, the controller immediately induces angular motion to counteract the minor orientation error.

The curves accelerate briefly before slowly decaying to zero angular velocity as the SACS approaches stability. This proves that under ideal conditions, the SACS correctly damps angular motion all whilst realigning the satellite. The lack if any residual angular rates in any principle axes also shows the SACS is able to stabilise and hold the satellite at the wanted orientation. The wheels reach a max speed of 0.25 radians per second well within the design specification.

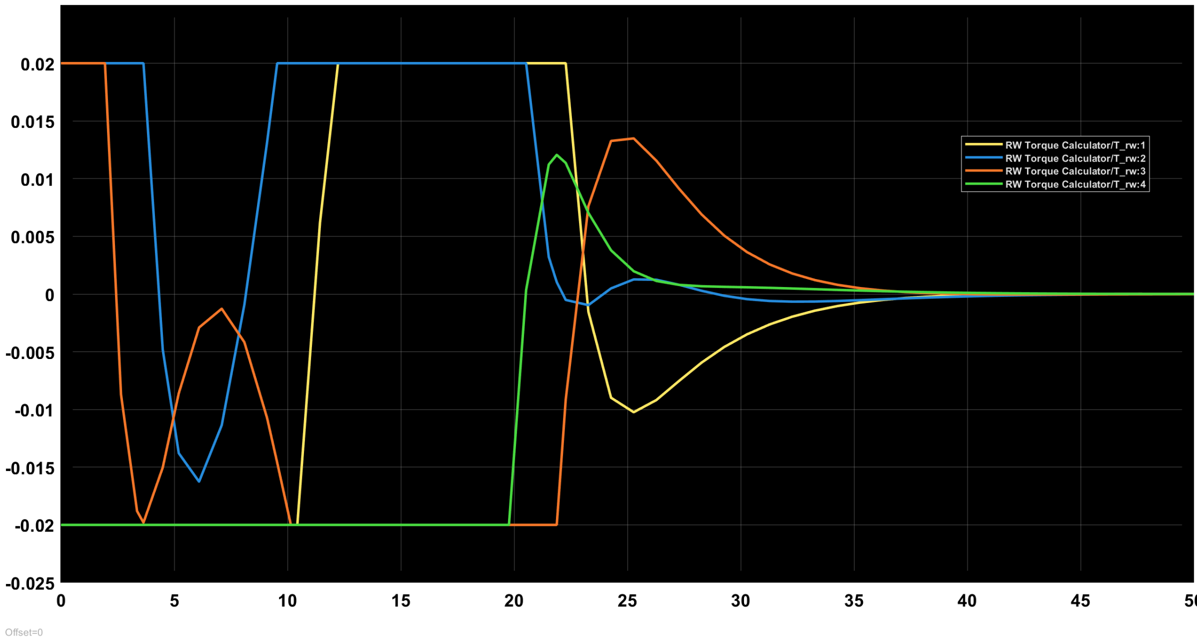

Figure 29: Reaction wheel Torque over time during small deviation test scenario.

Figure 29 details the torque applied on each reaction wheel as the SACS responds to the initial orientation error. The torque profile illustrates that torque is initially applied with some reaching the saturation torque which is well within the design specification.

As the quaternion error falls to stability, the torque applied to each wheel converges to zero. The smoothness of this waveform and lack of observations shows the controller applies energy sustainably and efficiently, and torque is only ever exerted when needed to correct orientation.

The proves adequate PD tuning giving a valid response time with no overshoot near the equilibrium (stability) point.

The results for Test 2 and 3 followed similar convergence trends as those shown in Test 1. In both cases, the quaternion error converged within specification with an angular error $> 0.05\circ$. Results can be seen in Table 15:

Test	**Settling Time (s)**	**Final Error (°)**	**Notes**
Test 2 – 90° Z direction	30	<0.05	Smooth convergence. Controller response was stable and within specification.
Test 3 – 180° X direction	33.7	<0.05	Successfully handled quaternion sign ambiguity. Longer settling time, but attitude stabilized without overshoot.

Table 15: Summary of Results for Operational Validation Tests 2 and 3

4.2.2 Disturbance Integration Test

This test evaluates the SACS against the internal,, time-varying disturbances generated by the motion of the satellite's arm and torques generated by environmental disturbances. Since the arm contributes a large amount of torque it is imperative the SACS can compensate for these effectively.

The arm torque (Figure 23) and environmental torque (see Figure 22) was injected into the system to confirm the functionality of the SACS during a typical repair mission. (assuming initial orientation must adjusted)

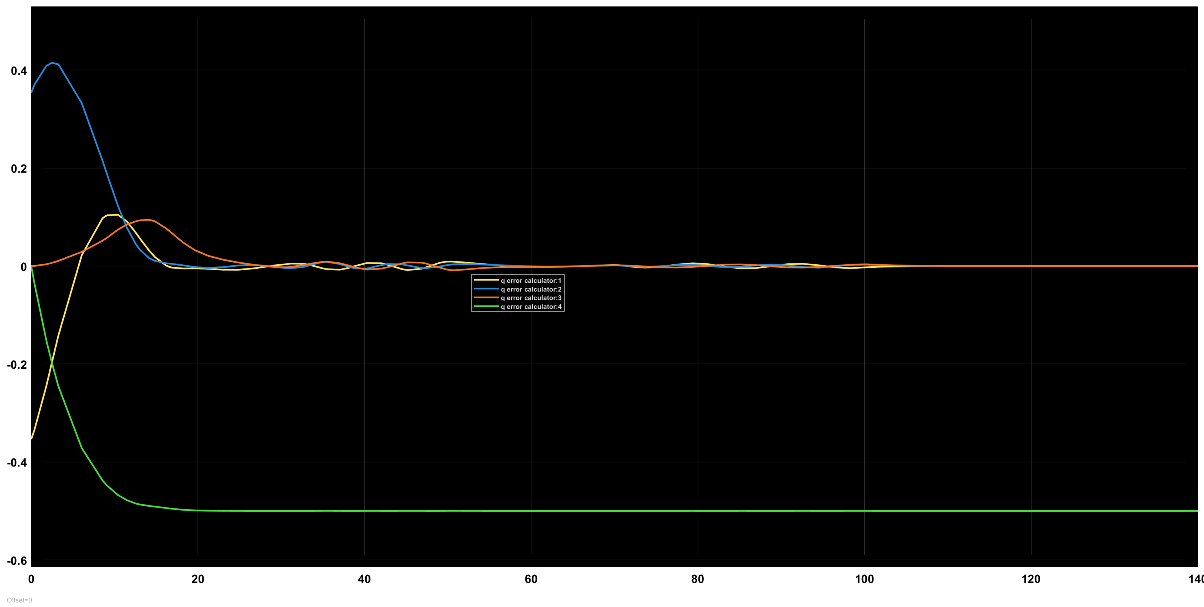

Figure 30: Error Quaternion In Presence Of Example Mission Repair

Figure 30 details as the arm moves throughout the repair mission, the SACS reacts throughout the mission time and after $\approx 30s$ the system reaches a rough stability as the reference quaternion (orientation) is reached and small adjustments are made to react to the arm disturbances.

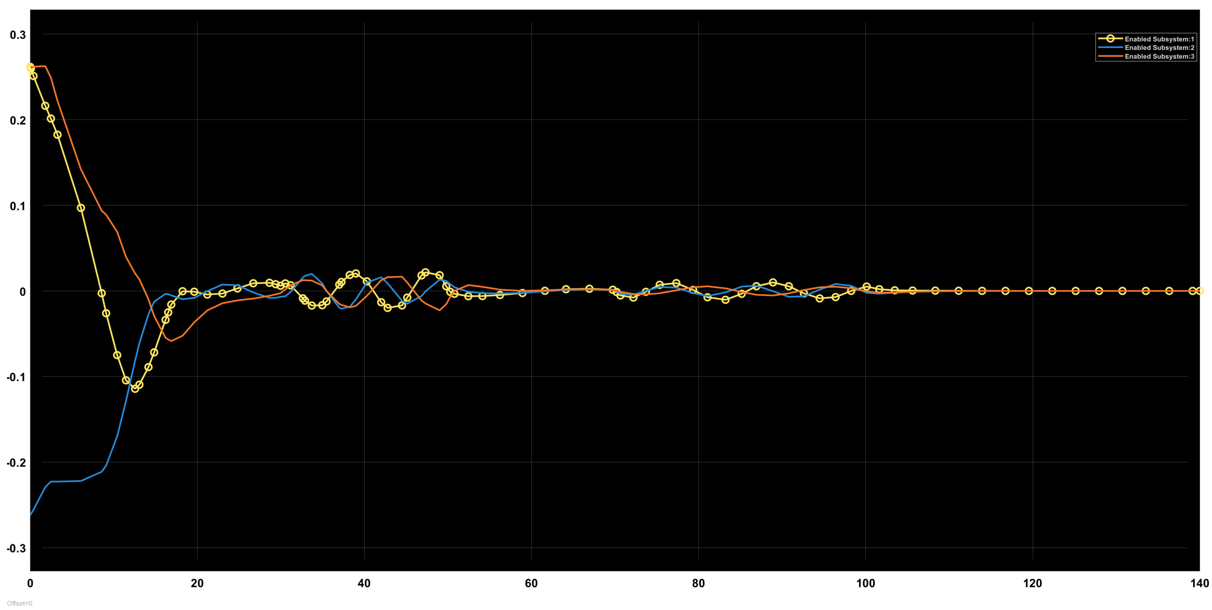

Figure 31: Angular Velocity In Presence Of Example Mission Repair

The satellites angular velocity is initially high as to translate to reference orientation before experiencing small adjustments to maintain attitude in the presence of the arm moving.

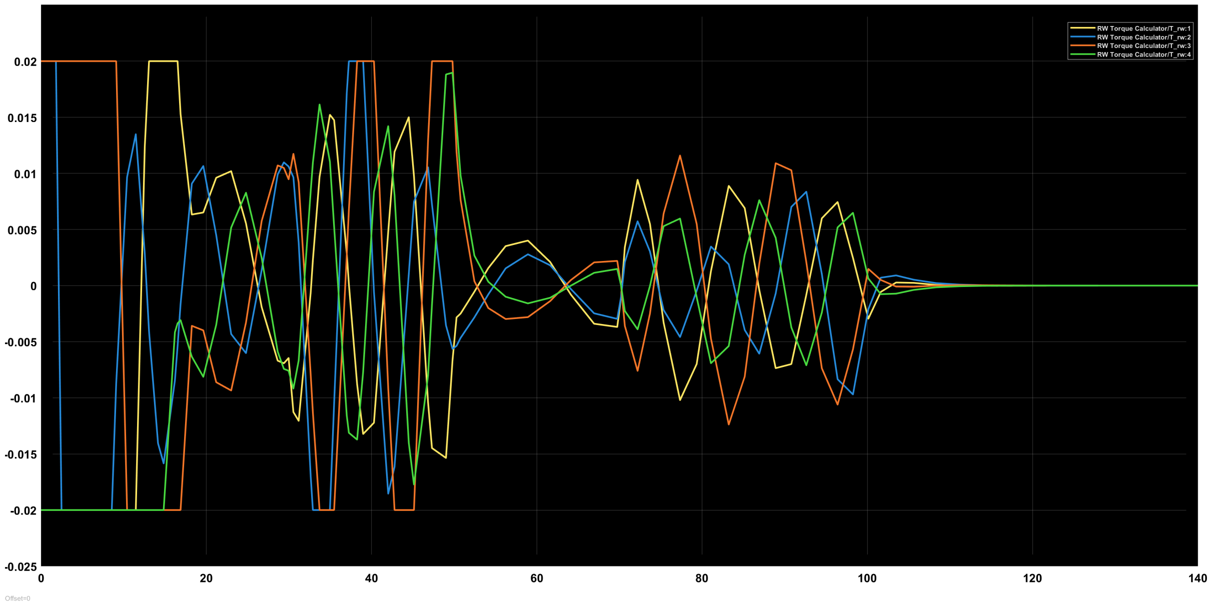

Figure 32: RW Torque In Presence Of Example Mission Repair

The Reaction wheel torque likewise operates perfectly and safety within the saturated parameters as seen in Figure 32. Perhaps more clearly defining the operational performance of the RWs, high torque is outputted initially (where the saturation occurrs) then is relatively small for the test of the repair mission as RWs aren't adjusting the attitude just reacting to the arm and environment disturbances until the repair is completed where the torque approaches zero.

The SACS performance is comparable to the ideal conditions even with such a wide array of disturbances. The pointing accuracy remains $< 0.05°$ (As a result of $|q_{e4}|$ approaching 0.5 or binary true), and no oscillations regardless of the amount of torque that can be expected to be applied by the repair process.

4.2.3 Redundancy Validation

It is likewise imperative to test the systems ability to maintain attitude when faced with an actuator (RW) failure. In the servicing mission redundancy is key such that if a failure takes place during a repair no further harm is done to the satellite. Likewise, redundancy makes the system commercially viable, aiding longer lifetimes.

Two fault conditions were simulated in isolation, with fault injection by disabling certain RWs in specific conditions

- **Single RW failure In Ideal Conditions:** Ensures SACS reacts as expected in ideal conditions.
- **Single RW failure While A Repair Is Being Done:** Ensures repair can still be completed despite of infant mortality of an actuator

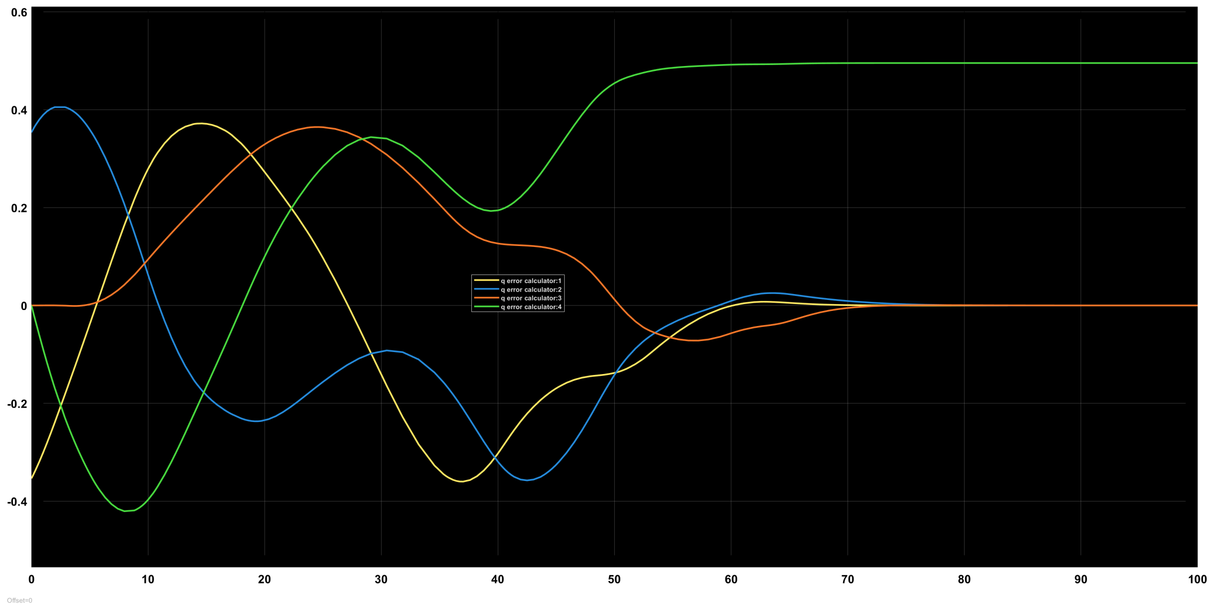

Figure 33: Quaternion Ideal Conditions With RW3 Failure

Figure 33 details the error quaternion ideal conditions with a complete failure of RW3 (no torque contribution), as can be seen, the SACS still reaches stability and correctly orientates that satellite. However, it take $\approx 70s$ double that of with four RWs to reach stability but still has very high accuracy of $< 0.05°$.

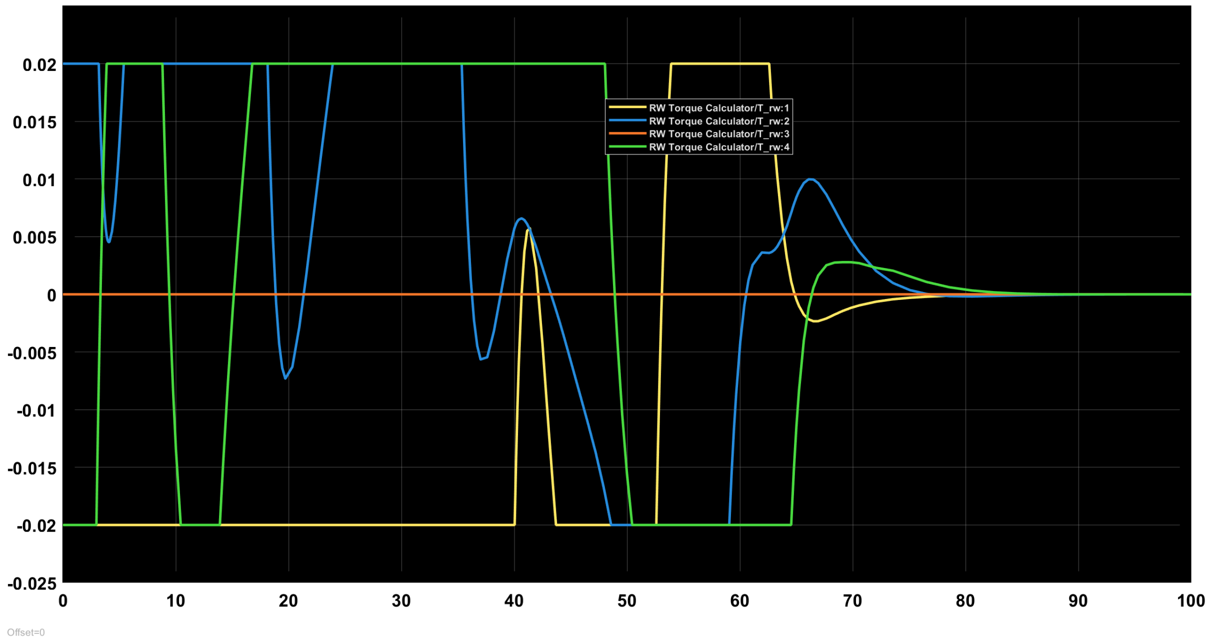

Figure 34: RW Torque In Ideal Conditions With RW3 Failure

As shown in Figure 34, the torque contribution of RW three is zero and the other three reaction wheels are saturated at the maximum allowed torque for longer in order to reach stability.

The SACS also reacts as expected to the disturbance caused by an expected mission (Figure 35 and Figure 36)

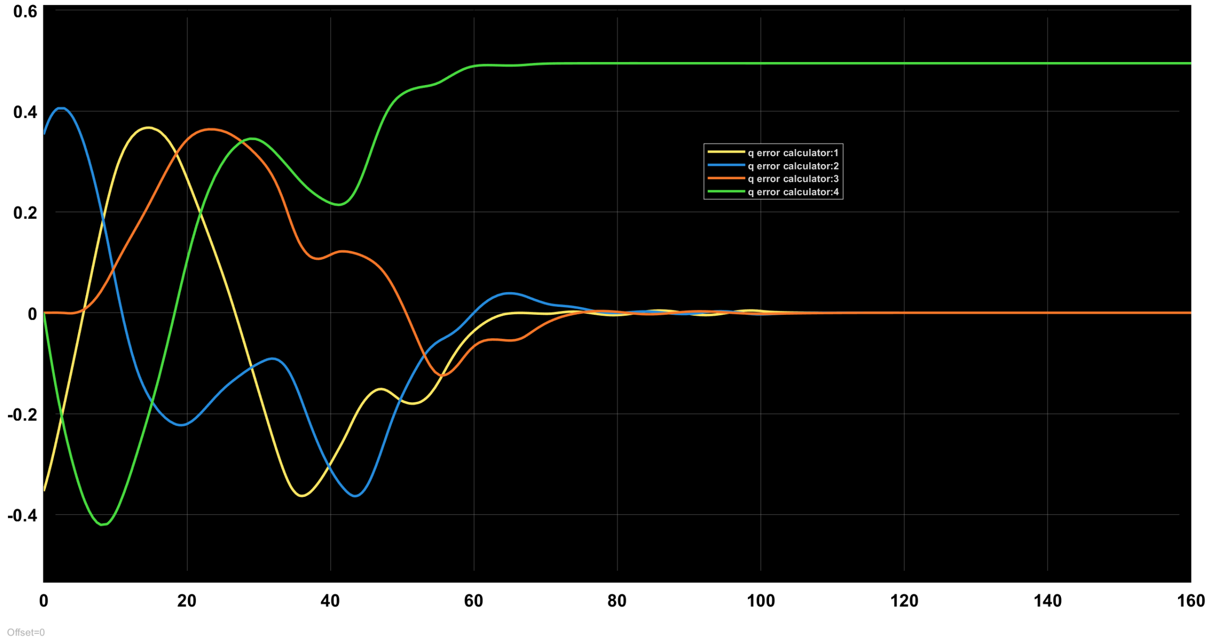

Figure 35: Quaternion Error With RW3 Failure During Mission

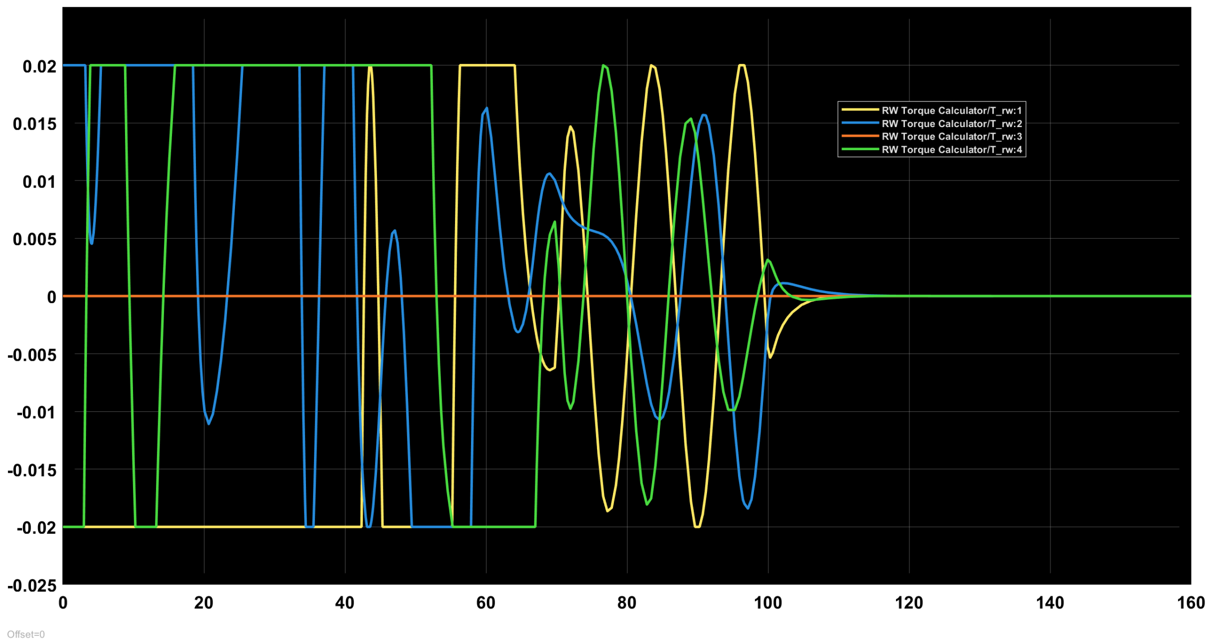

Figure 36: RW Torque In Repair Conditions With RW3 Failure

Thus, it can be seen that even in face of a critical failure during a repair, the correct torque and stability can be achieved for a safe repair, with no oscillations. All be it with reduced time to reach a pointing accuracy $< 0.05°$.

4.2.4 Micro-Thrusters Control Validation

The micro-thrusters burn must be tested such then when the wheels saturate, the micro-thrusters burn in an on/off method until stability is reached

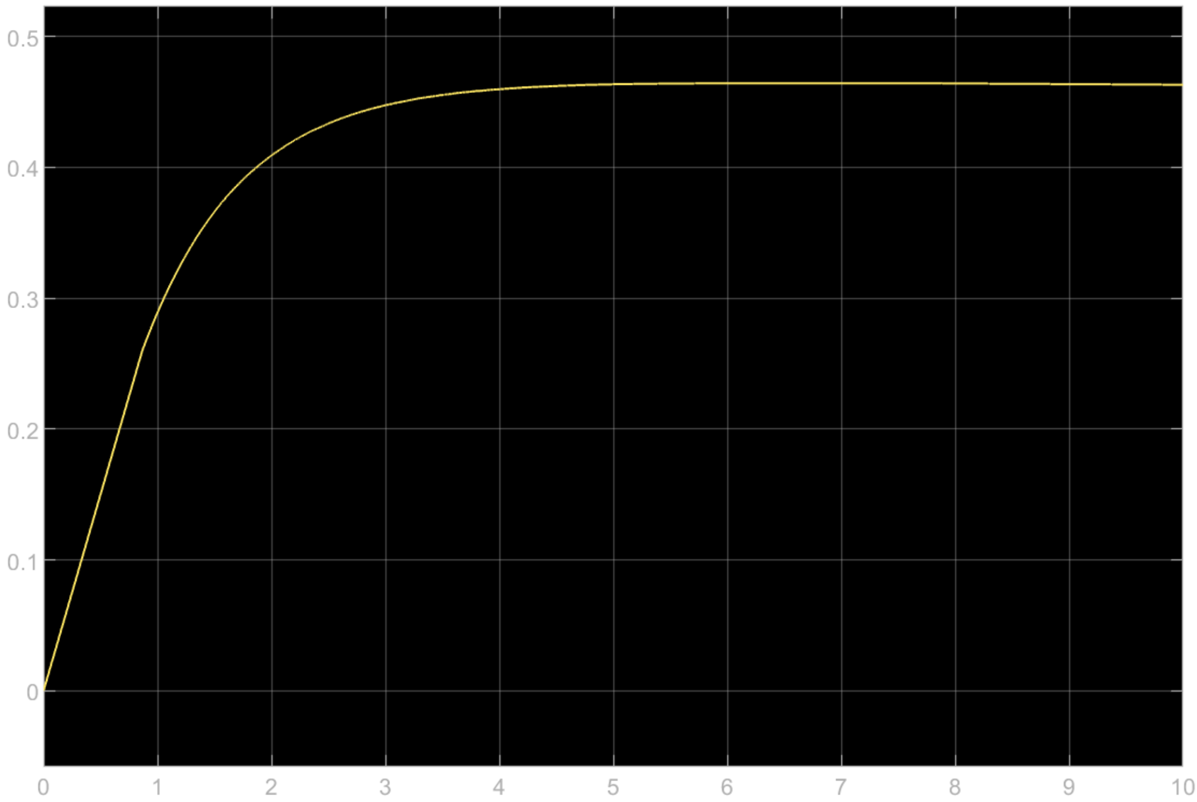

Figure 37: Stability Of Desaturation

The input is the required spin rate of the wheel in order to desaturate (in this case 0.45 radians per second) as can be seen in Figure 37, the Micro-thruster controller takes 4 seconds to reach stability.

The burn pattern and burn length can be seen in Figure 38.

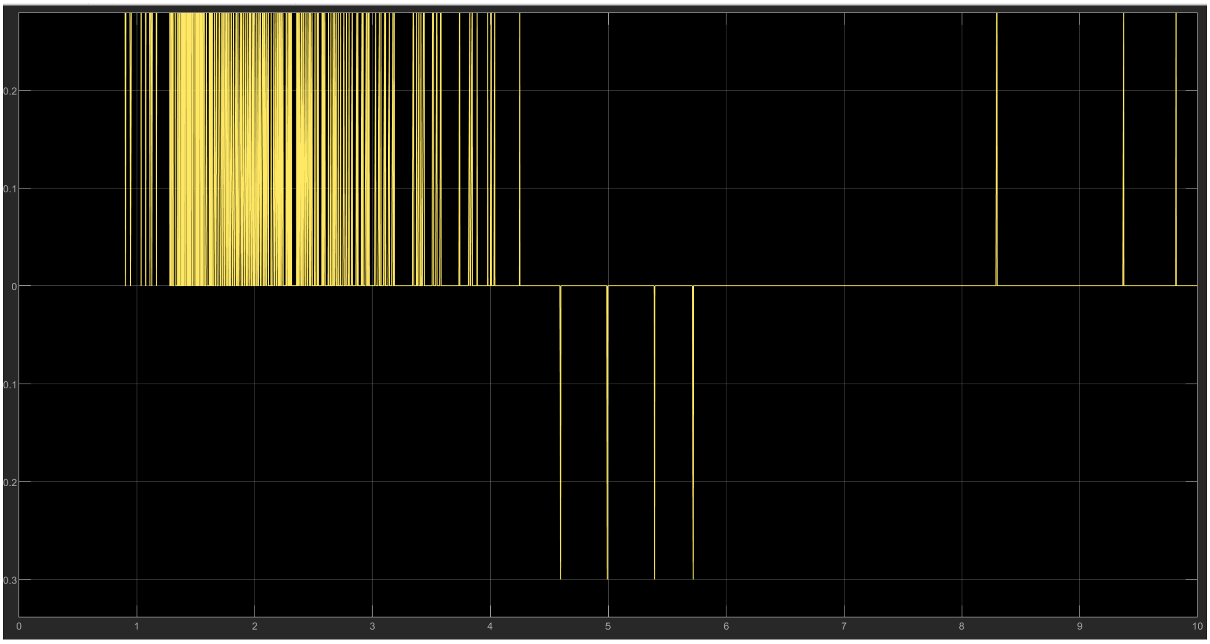

Figure 38: Thruster Burns During Desaturation

4.3 Mass And Power Calculations

Component	**Peak Power (W)**	**Mass (kg)**	**Reference**
Reaction Wheel (x4, Blue Canyon)	36 (9×4)	0.92 (0.24×4)	[9]
Sun Sensor (Aquila Fine Sun Sensor)	0.15	0.04	[31]
Gyroscope Sensor	0.05	0.03	[32]
Thruster System	14 (3.5 x 4)	4.5 (1.5 x 4)	[33]
Total	$< 50W$	**5.5 kg**	–

Table 16: Power and Mass Estimates for SACS Components with References

4.4 Design Specification Compliance

Functionally, the SACS completes all tests correctly and with high reliability.

The compliance of the SACS is compared with the predefined design specifications, the results of which are detailed in Table 17.

Specification	Target	Where Met	Pass/Fail
Pointing Accuracy	±0.05°	Achieved in steady-state during nominal and arm disturbance tests (see Figures 32, 29).	✓
Torque (Max Reaction Wheel)	±0.02 Nm	Confirmed in RW torque plots, this aligns with required manoeuvring torques.	✓
Response Time	75 s	System stabilised in $< 70s$ across all test cases, including singular RW failures.	✓
Peak Power Consumption	70 W Peak	Verified via subsystem power model and validated in energy consumption analysis (see Table **??**).	✓
Mass of SACS (Total)	10 kg	Verified via power calculations (Table 16)	✓
Alignment Tolerance (RWs)	2°	Shown in misalignment tolerance simulation using error quaternion analysis.	✓
Thruster Switching Time	0.1 s	Measured in Simulink event-driven actuation model.	✓

Table 17: Design Specification Compliance Summary for the 4-RW SACS

5 Solution Lifecycle

The lifecycle of the SACS, made up of four RWs with thrusters for desaturation, was evaluated in terms of costing, sustainability, procurement, logistics and maintainability in order to maintain mission success throughout the entire lifetime of the repair mission.

5.1 Costing

The complete bill of materials (BoM) was composed using real-world models and data sheets at market values for key components, the major cost include

- **Reaction Wheels:** £4,000–£7,000 per unit (e.g., Blue Canyon Technologies [9]).
- **Thrusters:** £3,000 per unit for compact monopropellant thrusters [33].
- **Sensors:** ≈£2,000 for a combined Sun tracker and Digital gyroscope ([31])
- **Onboard Computer and Drivers:** £5,000 including electronics(estimated).

- **Wiring, Harnessing, and Interfaces:** £1,000 estimated.
- **Software:** £2,000–£3,500 for MATLAB/Simulink licenses and real-time hardware ([34]).

Giving total estimated costs of ≈£30,000 to £40 000

In addition to the raw costs, it is integral to include a budget margin for integration, testing , PCB production (assumed tp be about 20%) bringing the total assumed cost to be around £60,000

5.2 Purchasing And Supply Chain

COTS (Commercial Off The Shelf Components) were chosen instead of custom made ones since for such a crucial task, since they already have established reliability and expected lifetimes. Risk of supply can be mitigated by identifying a list of secondary supplier ensuring multi-vendor compatibility such that if one vendor lacks the component, production does not have to stop. [Maybe find reference]. The lead times for specifically made components can be as long as 9 month thus using COTS components allow for ease in injection into satellite , especially important when trying to design a new standard. [35]

Using COTS likewise follows a modular integration plan with the SACS design itself, enhancing the maintainability and will facilitate future technological developments , reducing overall risks to the orbital service.

5.3 Logistics

The SACS due to the pyramidal shape is made to fit within a small to medium sized satellite. Due to the systems modularity and conformity to standards, the SACS actually imposes very minimal requirements on the satellite's power bus.

It is necessary logistically to test the SACS physical layout under vibration, vacuum and EMC testing in accordance to international standards.

5.4 Sustainability And Environmental

The core concept of the in-orbit repair service is to aid the future sustainability of space travel. Thus, it is imperative that the SACS remains with a max power draw of $< 70W$, aligning with most medium sized satellites. The implementation of the ON/OFF controller for thruster burnings likewise minimises the propellant used to desaturate the RWs.

The propulsion micro-thruster system itself can be implemented in the greenest way possible using green mono propellants[36] which is drastically less toxic than they hydrazine system used in many legacy satellite designs. Doing so, not only minimises the environmental impact within operation in space, but also mitigates the ground handling risks.

The system can be designed to support autonomous de-orbiting or refuelling autonomously adhering to standards, thus reducing the orbital debris generation to near zero (which is a key factor modern satellite mission must achieve).

5.5 Maintenance And Redundancy

Traditional satellite design have absolutely zero maintenance capability, but within the scope of this unique repair mission, it could be possibly implement a self repair/tweaking procedure that can meet future sustainability goals.

In addition to this, redundancy is a core part of the SACS design, The 4 RW pyramid shape, enables full control even with one wheel failure (as proven). In addition to this, the thruster array can be similarly configured such that nozzles can fail however momentum can still be dumped. Likewise, sensors are run with dual sensors hence if one was to fail orientation can still be established albeit less accurately.

6 Conclusion And Future Work

6.1 Project Summary And Design Specification Compliance

The design process of the SACS integrating a system of RWs and thrusters was completed with clear,concise and measurable design specifications, including, pointing accuracy, low power consumption, full three axis control all while adhering with sustainability goals set out by the goal of the in-orbit servicing mission. Each of these specifications and functional requirements were decomposed from the context of the in-orbit repair mission and design constraints that arise from the nature of the mission in the space environment.

Through rigorous simulation in Simulink, all imperative behaviours were confirmed and validated. The quaternion and Euler angle based controller showed consistent and fast convergence to desired orientations. With robust, empirical verification of the system response, torque and controller performance under a wide array of operation conditions in order to confirm all major functionality and design specifications were met (Section 4).

6.2 Project Management And Individual Contribution

As detailed in section 1. this project was done in a simple phased approach, starting with research , followed by subsystem definition, modelling, validating and final system performance validation.

From a technical standpoint, individually the complete design of a working SACS was completed including quaternion kinematics, real-world sensor and actuator modelling via data sheet information, modular Simulink blocks to simulate the disturbances.

Comprehensive models and documentation were employed to present clear traceability and enable repeatable tests for future iterations. Personal innovation and judgement were crucial in identifying and tackling limitation in early models and adapting seamlessly to changing test results.

6.3 Risk Management

Risk was managed and controlled throughout the design process.Significant risk are encountered throughout the design of an SACS whether it be from Arm or external disturbances.

Conflicts between constraints particularly weight, redundancy and power were resolved through careful trade-off analysis, documented in the specific selection criteria (section 2).

Where system-level conflicts could not be resolved (i.e thruster configuration) recommendations were defined to guide further endeavours into completing the platform design, making the risk of integrating the designed SACS minimal and modular to most platforms.

6.4 Future Work

Whilst all the core objectives of this sub system were met, several key factor present themselves that offer future refinement and expansion.

Primarily, translation control during the docking procedure. A key plan was defined (See Appendix x) but future work should incorporate translational dynamics which enable full autonomous docking, using propulsion to perform alignment based on contact based (docking) meanderers.

Secondly, as is the nature of Simulink , whilst the control system is designed , it cannot be tested in real-time thus testing in a real-time system will be needed before implementation which can further test efficiency, latency and real-time response to faults.

In addition, whilst the control system can continue in the presence of faults, currently there's no onboard detection software for what specific fault has taken place. This can incorporate the ever advancing field of machine learning in conjunction with the concept of self-repair to produce an even more sustainable In-orbit serving satellite.

6.5 Final Reflection

Overall, this project has outputted a robustly tested, modular SACS that is capable of achieving stability in an in-orbit scenario. It has met all defined requirements, implemented complex yet functional systems with good engineering practices perhaps more critically, allowing for further real-world testing and project expansion. Throughout, key conflict resolution, problem solving and innovation has been shown.

Acknowledgments

I would like to sincerely thank Biagio Forte, for his guidance and continued support throughout the semester. I'm also grateful for my team mates who excellent problem solving and engagement has made the entire project very enjoyable. Working together on such a exciting project together made this not just a valuable learning experience but also a lot of fun.

In addition to this, I acknowledge generative AI tools (specifically OpenAIs ChatGPT), were used during the initial preparing stages of this report to explore the background of the task , and suggest directions for initial research likewise assist in condensing draft content. I take full responsibility and ownership for the accuracy, originality and integrity of this submitted content.

References

[1] K. Barnett. *What happens to satellites that run out of power?* Geographic FAQ Hub: Answers to Your Global Questions. 2024. URL: https://www.ncesc.com/geographic-faq/what-happens-to-satellites-that-run-out-of-power/#:~:text=As%20of%20current%20records%2C%20there%20are%20over%203%2C000,objects%2C%20including%20fragments%20and%20remnants%20of%20space%20missions...

[2] Iotbyhvm. *What is an Actuator? Types, Principles, and Applications*. Iotbyhvm. 2024. URL: https://www.nextpcb.com/blog/What-is-an-actuator-types-principles-and-applications.

[3] *Attitude sensors - supply chain hub*. Satsearch, Published: Feb. 26, 2025. Accessed: May 22, 2025. 2025. URL: https://satsearch.co/attitude-sensors.

[4] R. Y. *Attitude Control system*. Electronics Desk. 2021. URL: https://electronicsdesk.com/attitude-control-system.html.

[5] A. Montemaggi. *What Exactly Are the Forces that Act Upon a Satellite?* Science Capsule, impulso.space. 2023. URL: https://impulso.space/tools/blog/posts/what-exactly-are-the-forces-that-act-upon-a-satellite.

[6] A. Bitar. *Understanding reaction wheels*. Honeywell Aerospace Blog. n.d. URL: https://aerospace.honeywell.com/us/en/about-us/blogs/understanding-reaction-wheels.

[7] *10.7 Newton's Second Law for Rotation - University Physics Volume 1*. OpenStax. n.d. URL: https://openstax.org/books/university-physics-volume-1/pages/10-7-newtons-second-law-for-rotation.

[8] NSE. *Satellite Components: Reaction Wheels*. New Space Economy. 2023. URL: https://newspaceeconomy.ca/2023/10/24/satellite-components-reaction-wheels/.

[9] *Blue Canyon Technologies • REACTION WHEELS*. Blue Canyon Technologies. 2025. URL: https://www.bluecanyontech.com/wp-content/uploads/Reaction-Wheels-1_2025.pdf.

[10] T. V. Cherd, R. Daud, and S. Yaacob. "Optimal control of a tetrahedral configured reaction wheels for Quaternion rotation based on rigid satellite model". In: *IOP Conference Series: Materials Science and Engineering*. Vol. 670. 2019, p. 012033. DOI: 10.1088/1757-899x/670/1/012033.

[11] M. Nehrenz and M. Sorgenfrei. *A Comparison of Thruster Implementation Strategies for a Deep Space Nanosatellite*. Tech. rep. NASA, 2019. URL: https://ntrs.nasa.gov/api/citations/20190001651/downloads/20190001651.pdf.

[12] *BGT-X5 Green Monopropellant Thruster*. BGT Datasheet. n.d. URL: https://static1.squarespace.com/static/60df2bfb6db9752ed1d79d44/t/61292af2a097083a87c4cbc0/1630087925107/BGT_X5_v1.0.pdf.

[13] J. Amin. *The Design, Assembly, and Testing of Magnetorquers for a 1U CubeSat Mission*. Tech. rep. Georgia Institute of Technology, 2019. URL: https://repository.gatech.edu/server/api/core/bitstreams/db0bd935-ce1c-4f55-a4af-d4c9655a0a41/content.

[14] Matan. *How magnetorquer rods work in satellites — Description, Example and Application*. Your Physicist. 2023. URL: https://your-physicist.com/how-magnetorquer-rods-work-in-satellites/.

[15] *NCTR-M002 NCTR-M012 NMTR-X [Custom]*. CubeSat Shop. URL: https://www.cubesatshop.com/wp-content/uploads/2016/06/NewSpace-Magnetorquer-Rod_7b.pdf.

[16] NSE. *Satellite Components: Control Moment Gyroscopes*. New Space Economy. 2024. URL: https://newspaceeconomy.ca/2024/10/21/satellite-components-control-moment-gyroscopes/.

[17] James Richard Wertz and Computer Sciences Corporation. *Attitude Systems Operation, Spacecraft Attitude Determination and Control*. Dordrecht: Kluwer Academic Publishers, 1978.

[18] GyroPlacecl.com. *Control Moment Gyroscope vs Reaction Wheel: A Comprehensive Comparison*. GyroPlacecl.com. 2023. URL: https://gyroplacecl.com/control-moment-gyroscope-vs-reaction-wheel-a-comprehensive-comparison/.

[19] *M50 Control Moment Gyroscope (CMG)*. Honeywell. URL: https://satcatalog.s3.amazonaws.com/components/6/SatCatalog_-_Honeywell_-_M50_CMG_-_Datasheet.pdf?lastmod=20210708012029.

[20] *What is a Sun Sensor?* AZoSensors.com. 2013. URL: https://www.azosensors.com/article.aspx?ArticleID=223.

[21] *AI-SES IR Earth Sensor - Earth/Horizon Sensor*. SatCatalog. URL: https://www.satcatalog.com/component/ai-ses-ir-earth-sensor/.

[22] Amin Ali Mody et al. "Attitude Determination and Control System Design for Srmsat-2: A Micro Class Lunar Orbiter". In: *55th AIAA Aerospace Sciences Meeting*. 2017. DOI: 10.2514/6.2017-0165.

[23] H. Song, S. L. Hu, and W. Z. Chen. "Simulink-based simulation platform design and faults impact analysis of attitude control systems". In: *The Aeronautical Journal* 126.1297 (2021), pp. 475–499. DOI: 10.1017/aer.2021.79.

[24] A. Kasiri, F. F. Saberi, and Mehdi Kashkul. "Optimization of Pyramidal Reaction Wheel Configuration for Minimizing Angular Momentum". In: *Proceedings of ICCIA*. 2021. DOI: 10.1109/iccia52082.2021.9403596.

[25] A. Bani Younes and D. Mortari. "Derivation of All Attitude Error Governing Equations for Attitude Filtering and Control". In: *Sensors* 19.21 (2019), p. 4682. DOI: 10.3390/s19214682.

[26] L. You, Y. Dong, and X. Bing. "PD-like finite time controller with simple structure for satellite attitude control". In: *Defence Technology* 26 (2022), pp. 123–133. DOI: 10.1016/j.dt.2022.06.004.

[27] A. Khosravi and P. Sarhadi. "Tuning of Pulse-Width Pulse-Frequency Modulator using PSO: An Engineering Approach to Spacecraft Attitude Controller Design". In: *Automatika* 57.1 (2016), pp. 212–220. DOI: 10.7305/automatika.2016.07.618.

[28] T. Cilliers, W. H. Steyn, and H. W. Jordaan. "Multi-axis thruster-only fine pointing control strategies for nanosatellites". In: *Aerospace Science and Technology* 150 (2024), p. 109247. DOI: 10.1016/j.ast.2024.109247.

[29] S. A. Chee, J. R. Forbes, and D. S. Bernstein. “Gravity-gradient-stabilized spacecraft attitude estimation using rate-gyroscope measurements”. In: *2022 American Control Conference (ACC)*. 2016, pp. 7067–7072. DOI: 10.1109/acc.2016.7526787.

[30] admin cleanenergybusinesscouncil. *Solar Radiation Pressure - Definition & Detailed Explanation - Solar Energy Glossary Terms*. CleanEnergyBusinessCouncil.com. 2024. URL: https://cleanenergybusinesscouncil.com/solar-energy-glossary/solar-radiation-pressure/.

[31] *Sun Sensor*. NewSpace Systems. n.d. URL: https://www.newspacesystems.com/products/sun-sensors/.

[32] *L3GD20H - MEMS motion sensor: three-axis digital output gyroscope*. STMicroelectronics, Gyroscope Datasheet. n.d. URL: https://www.pololu.com/file/0J731/L3GD20H.pdf.

[33] *Delivers 0.5N of thrust and 565N-s of impulse in a 1U CubeSat volume*. Benchmark Space Systems, BGT-X5 Datasheet. n.d. URL: https://static1.squarespace.com/static/60df2bfb6db9752ed1d79d44/t/61292af2a097083a87c4cbc0/1630087925107/BGT_X5_v1.0.pdf.

[34] *Pricing and Licensing*. MathWorks. n.d. URL: https://uk.mathworks.com/pricing-licensing.html.

[35] BIS Research. *Satellite Commercial-off-the-Shelf Components Enabling Innovation in Space Technology*. BIS Research, Accessed: May 23, 2025. 2022. URL: https://bisresearch.com/news/satellite-commercial-off-the-shelf-components-enabling-innovation-in-space-technology-.

[36] Dawn Aerospace. *Dawn Aerospace*. Dawn Aerospace, Accessed: May 23, 2025. 2025. URL: https://www.dawnaerospace.com/green-propulsion-2025.

Appendix A- Needs Analysis

Needs analysis	
Ref Need	Description
Technical Needs	
N1	Must be able to secure a damaged satellite
N2	Must be able to identify and locate damaged component
N3	Must be able to remove damaged component and store it along with any fixings (screws etc)
N4	Must be able to replace and secure a new component in the same location.
N5	Must use COTS components for demonstrator which follow the relevant standards (DSTL)
Commercial Needs	
N6	Must be cost effective for users and owners of damaged satellite (cost less to repair than to relaunch)
N7	Must be effective for a specified range of satellite types and/or subsystems of the satellites
N8	Must have a way of recycling or disposing of damaged components - maybe return to Earth.
N9	Must be economically viable as a service and/or product.
Ethical Needs	
N10	Must not contribute further to space debris.
N11	Political considerations - maintain the collabrative nature of space technologies.
N12	Must conform to ethical business practices in view of a broader interest from DSTL

Appendix B- Target Specification

Ref Spec	Description	Objectives measurable + tolerance
SP1.1	Satellite being repaired must not be able to be displaced in any direction by more than a specified amount	+/- 5% of longest dimension of platform performing repair
SP1.2	Must maintain attitude control (and perform stationkeeping) for duration of repair	Produce simulations to confirm max satellite mass that can be secured
SP2.1	Must identify a point in space which corresponds to the center of the damaged component	center point has a tolerance of +/-5% of the longest dimension of damaged component
SP2.2	Repeatable recognition of damaged component	Success rate of 95%
SP3.1	Ensure system is capable of modular variation in order to handle various component types/sizes	
SP4.1	Identify component type (Part Number)	Success rate of 95%
SP4.2	Identify suitable replacement	Success rate of 95%
SP4.3	Replace and secure replacement component in same location.	center point has a tolerance of +/-5% of the longest dimension of damaged component Success rate of 95%
SP4.4	Provide safe transportation for replacement component by conforming to satellite shielding standards	
SP4.5	Method of repair must not impede long term satellite functionality/lifetime	
SP5.1	Ensure the components adhere to the relevant standards as outlined by Space Agencies (ESA in particular)	IEEE, ECSS (Space Standardisation), ECSL (European Space Law), NTSS (US standard), ISO
SP6.1	Must cost less for customers to use our product/service than to replace entire satellite.	Cost of Repair < Cost to Replace.
SP7.1	Solution should be scaleable to operate on satellites of varying size and value above a margin of profitability	
SP7.2	Solution should be able to operate in both LEO and GEO orbits.	
SP8.1	Must collect and store damaged components	Chance of contributing space debris of any size should be < 10% Chance of contributing space debris of size >1cm^3 should be < 5%
SP9.1	Must at least break even on cost	
SP10.1	Must not exceed maximum volume. Vehicle itself must not become debris	Chance of contributing space debris of any size should be < 10% Chance of contributing space debris of size >1cm^3 should be < 5%
SP11.1	Keep mission plans transparent to avoid concerns of sabotage.	

Figure 40: Target Spec

Appendix C- Example Idea Conceptualisation

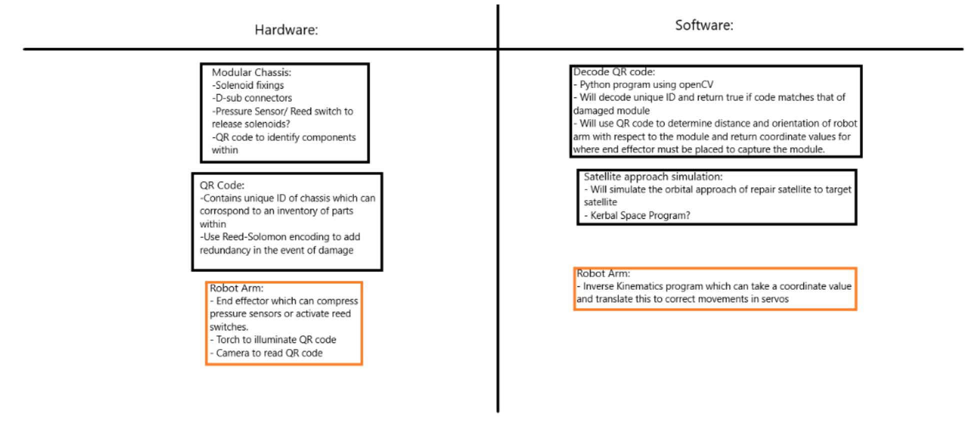

Figure 41: Concept 1

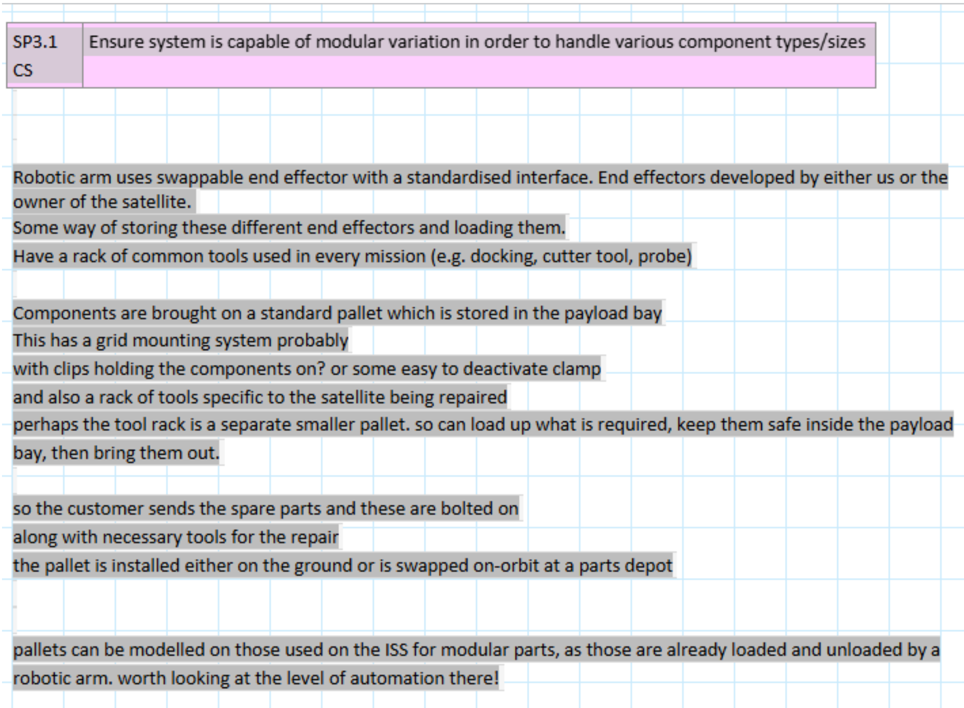

SP3.1 CS	Ensure system is capable of modular variation in order to handle various component types/sizes

Robotic arm uses swappable end effector with a standardised interface. End effectors developed by either us or the owner of the satellite.
Some way of storing these different end effectors and loading them.
Have a rack of common tools used in every mission (e.g. docking, cutter tool, probe)

Components are brought on a standard pallet which is stored in the payload bay
This has a grid mounting system probably
with clips holding the components on? or some easy to deactivate clamp
and also a rack of tools specific to the satellite being repaired
perhaps the tool rack is a separate smaller pallet. so can load up what is required, keep them safe inside the payload bay, then bring them out.

so the customer sends the spare parts and these are bolted on
along with necessary tools for the repair
the pallet is installed either on the ground or is swapped on-orbit at a parts depot

pallets can be modelled on those used on the ISS for modular parts, as those are already loaded and unloaded by a robotic arm. worth looking at the level of automation there!

Figure 42: Concept 2

SP7.1 TP	Solution should be scalable to operate on satellites of varying size and value above a margin of profitability	

Modular system for easy scalability:

- Advantages:
  - Easy to scale up by changing specific parts to match the specific project
  - Cost effective as bespoke parts aren't needed for all parts
- Disadvantages:
  - Can be bad for highly specialised repairs (might just not be able to complete repairs over a certain complexity)

Custom designed repairs satellite:

- Advantages:
  - Good for more specialised repairs so can allow repairs of more complex satellites
- Disadvantages:
  - Much less cost effective

Figure 43: Concept 3